



**HAL**  
open science

## Optimization of the growth and marennine production by the diatom *Haslea ostrearia* in photobioreactor

R Nghiem Xuan, J Mouget, V Turpin, P Jaouen, Jeremy Pruvost

► **To cite this version:**

R Nghiem Xuan, J Mouget, V Turpin, P Jaouen, Jeremy Pruvost. Optimization of the growth and marennine production by the diatom *Haslea ostrearia* in photobioreactor. *Algal Research - Biomass, Biofuels and Bioproducts*, 2021, 55, 10.1016/j.algal.2021.102251 . hal-03609181

**HAL Id: hal-03609181**

**<https://hal.science/hal-03609181>**

Submitted on 15 Mar 2022

**HAL** is a multi-disciplinary open access archive for the deposit and dissemination of scientific research documents, whether they are published or not. The documents may come from teaching and research institutions in France or abroad, or from public or private research centers.

L'archive ouverte pluridisciplinaire **HAL**, est destinée au dépôt et à la diffusion de documents scientifiques de niveau recherche, publiés ou non, émanant des établissements d'enseignement et de recherche français ou étrangers, des laboratoires publics ou privés.

# Optimization of the growth and marennine production by the diatom *Haslea ostrearia* in photobioreactor

R. Nghiem Xuan<sup>a,b</sup>, J.L. Mouget<sup>b,c</sup>, V. Turpin<sup>b</sup>, P. Jaouen<sup>a</sup>, J. Pruvost<sup>a,\*</sup>

<sup>a</sup> Université de Nantes, Oniris, CNRS, GEPEA, UMR 6144, F-44600, France

<sup>b</sup> Université de Nantes, MMS, EA 2160, Faculté des Sciences et des Techniques, 2 Rue de la Houssinière, BP, 92208, 44322 Nantes Cedex, France

<sup>c</sup> MMS (Mer Molécules Santé), Le Mans Université, Ave O. Messiaen, 72085 Le Mans, France

## ARTICLE INFO

### Keywords:

Microalgae  
Photobioreactor  
*Haslea ostrearia*  
Marennine  
Culture  
Optimization

## ABSTRACT

The benthic diatom *Haslea ostrearia* which has the capacity to excrete a blue pigment called marennine remains a challenging organism to culture in a photobioreactor (PBR). This study investigates the interest of culture in conventional mixed PBR over immobilized-cell protocols which proved successful but have rather low extracellular marennine (EMn) due to a limitation in mass or light transfer in the biofilm. In contrary, culture in mixed PBR has been proven to overcome culture mass transfer limitation, and to provide a high level of control over light access to cells, enabling the application of systematic optimization of photosynthesis-related kinetics.

Increasing the dissolved inorganic carbon concentration up to values of around 5–10 mM was found to increase both growth kinetics and EMn production. Growth medium enrichment with silica (Si) was however found to be challenging due to chemical precipitation. A fed-batch strategy on Si-P supply was implemented, leading to an increase in biomass productivity ( $51.8 \pm 2.3 \text{ mg}_X \text{ L}^{-1} \text{ d}^{-1}$ ). Although EMn was produced continuously, the nutrient-limited conditions led to higher productivity with  $9.2 \pm 1.7 \text{ mg}_{\text{EMn}} \text{ m}^{-2} \text{ d}^{-1}$ ,  $37.9 \pm 0.7 \text{ mg}_{\text{EMn}} \text{ m}^{-2} \text{ d}^{-1}$  and  $54.5 \pm 1.8 \text{ mg}_{\text{EMn}} \text{ m}^{-2} \text{ d}^{-1}$  for phosphorus, silicon and nitrogen deprivation respectively.

The effect of light availability was also investigated, as represented by the Mean Rate of Photon Absorption (MRPA). A direct relation was shown for both biomass and EMn production kinetics. However, maximal biomass and EMn productivities were found at different MRPA values, respectively  $1.7 \pm 0.1 \text{ g}_X \text{ m}^{-2} \text{ d}^{-1}$  at  $12.3 \mu\text{mol}_{\text{hv}} \text{ g}_X^{-1} \text{ s}^{-1}$  and  $11.0 \pm 0.5 \text{ mg}_{\text{EMn}} \text{ m}^{-2} \text{ d}^{-1}$  at  $8.4 \mu\text{mol}_{\text{hv}} \text{ g}_X^{-1} \text{ s}^{-1}$ .

Finally, a continuous EMn production was obtained in optimal conditions, leading to a productivity of  $4.5 \pm 0.16 \text{ mg}_{\text{EMn}} \text{ L}^{-1} \text{ d}^{-1}$ , enabling validation of the conventional mixed PBR for *H. ostrearia* culture and continuous EMn production.

## 1. Introduction

Microalgae are investigated for industrial purposes due to their potential for producing molecules for pharmacology, cosmetology, food and biofuel, and for their use in water treatment and CO<sub>2</sub> valorization [1,2]. Nowadays however there are few industrialized microalgae, representing only a minor part of algae biodiversity. There are estimated to be about 200,000–800,000 species of which only 50,000 have been described [3]. This could be partly due to difficulties in scaling-up the culture to industrial levels. A significant lack of knowledge is usually the main reason [1], but in the case of diatoms and dinoflagellates, high sensitivity to hydrodynamic shear stress and stirring conditions is often referenced [4]. Additionally, specific culture medium and culture

conditions may be required, as has previously been shown for several species cultivated on a large scale. This is the case with *Haematococcus pluvialis* for astaxanthin production, obtained under intense light, high salinity, and low availability of nutrients [5,6], and for *Dunaliella salina* production of β-carotene, obtained under intense light and high salinity [7,8].

*Haslea ostrearia* is a diatom that has been studied since 1820 [9] at laboratory scale. It has the capacity to produce and excrete a blue pigment called marennine, which has industrial potential [10]. Culture has already been demonstrated at relatively large volume. Gastineau et al. [11] for example obtained a concentration  $7 \text{ mg}_{\text{EMn}}/\text{L}$  in a 100 L culture system operated in batch mode. This microalgae strain is well known to be shear-stress sensitive [12] and its culture in PBR conditions

remains therefore challenging. Culture in a specific photobioreactor (PBR), such as agar immobilization PBR and immersed membrane PBR [13,14], was implemented. The approach was successful due to the benthic behavior of *H. ostrearia*. Cell immobilization also enabled the prevention of hydrodynamic shear stress on cells [15,16], but although immobilized-cell protocols proved successful, the extracellular marennine production obtained was fairly low, i.e.  $0.63 \pm 0.05 \text{ mg}_{\text{EMn}} \text{ L}^{-1} \text{ d}^{-1}$  and  $0.43 \pm 0.05 \text{ mg}_{\text{EMn}} \text{ L}^{-1} \text{ d}^{-1}$  for passive immobilized cell and agar gel immobilization respectively. This can be attributed to limitations in mass or light transfer in the biofilm, thereby decreasing the kinetics of biosynthesis (i.e. growth and EMn production).

Medium composition and cell fragility have been investigated in a previous work [17] A new NX medium was proposed and it was demonstrated that *H. ostrearia* cells could tolerate mixing conditions when an appropriate stirring strategy was applied. This opens up the perspective of a systematic optimization of culture conditions. As already demonstrated in several publications [18,19], suspended-cell culture enables the prevention of growth limitation by nutrient access (including dissolved organic carbon) while optimizing photosynthetic growth by controlling light availability in bulk.

The aim of this work is to investigate and optimize the parameters (pH, temperature and light) for *H. ostrearia* culture in a mixed PBR. Comparison will be made with immobilized cell culture. The influence on Extracellular Marennine (EMn) productivity will also be considered. Currently, the EMn production pathway remains unclear. Robert [20] attested that EMn is continuously produced as a primary metabolite, whereas Neuville and Daste [21], Rossignol [13] and Lebeau [14] indicated an increased production under nitrogen deprivation. Both strategies will be investigated here.

## 2. Materials and methods

### 2.1. Culture media for production in PBR

The ES 1/3 medium [20] modified with the same molar amount of inorganic sources of phosphorus ( $\text{KH}_2\text{PO}_4$ ) and carbon ( $\text{NaHCO}_3$ ) was used for the following part of the study [17]:

- Immobilized *H. ostrearia* cell culture
- Nutrient consumption in PBR culture
- Establishing the optimal growth parameters for biomass and EMn production

The final optimization was carried out using NX artificial seawater medium [17]. This medium was designed for *H. ostrearia* culture in artificial seawater, in order to control the medium composition and increase the macronutrient concentration without precipitation/limitation phenomenon. Note that this medium was not used for all the experiments because previous experiments were carried out before it was available.

### 2.2. Cell density and biomass concentration measurement

Cell density measurement was carried out by counting the cells using a Nageotte counting chamber (Marienfeld, AQRA, India) and observed by light microscopy (AXIO Scope A1, Zeiss, Germany). Dry weight measurement was carried out by filtering a 10 mL sample on 0.7  $\mu\text{m}$  Whatman GF/F. The same volume of ammonium formate ( $\text{NH}_4\text{HCO}_2$  at  $28 \text{ g L}^{-1}$ ) was added in order to remove the salt weight. The filters were then desiccated over 24 h at  $110^\circ\text{C}$ .

### 2.3. Determination of pigment concentration

The measurement of pigments, chlorophylls *a*, *c* and total carotenoids, were carried out with the acetone 90% extraction protocol by the Ritchie [22] protocol, and carotenoids by the Strickland and Parsons

[23] protocol. 1 mL of culture sample in glass container is centrifuged 15 min at 4000g with MiniSpin®. After supernatant elimination, 1 mL of 90% acetone is added and put during 3 h at  $3^\circ\text{C}$  and obscurity. The extracted pigment solution was measured (480, 630, 647 and 664 nm) by spectrophotometer (V-630 UV-VIS, JASCO, Germany). The extracellular marennine (EMn) was measured by a spectrophotometer (V-630 UV-VIS, JASCO, Germany) in the supernatant after centrifugation of the sample. A wavelength of 669 nm was selected and the EMn mass concentration measured using the Beer-Lambert equation ( $\epsilon = 12 \times 10^4 \text{ mol L}^{-1} \text{ cm}^{-1}$  and  $M_{\text{EMn}} = 9893 \text{ Da}$ ) according to Pouvreau et al. [24].

### 2.4. Nutrient concentration measurement

Nitrogen and phosphorus were mainly measured by ion chromatography (DIONEX ICS 1100 cationic column and ICS 900 anionic column, Thermo-scientific, France). Analyses were conducted immediately after sampling the culture. 5 mL sample were filtrated into 0.2  $\mu\text{m}$  before being injected into the ion chromatography. Silicon nutrient was measured by silicon-molybdate colorimetric methods [25]. A high concentration of extracellular marennine interferes with this colorimetric reaction and produces an overestimation. Dissolved Inorganic Carbon (DIC) was measured by catalytic oxidation methods by combustion at  $680^\circ\text{C}$ , using a Total Organic Carbon analyzer (TOC-L CSH/CSN, Shimadzu, UK).

### 2.5. Determination of the Mean Rate of Photon Absorption (MRPA)

The Mean Rate of Photon Absorption, also denoted "A", refers to the light absorbed by cells per unit of time and microalgal biomass. It is expressed in  $\mu\text{mol}_{\text{hv}} \text{ kg}_x^{-1} \text{ s}^{-1}$  [26,27,28]. The MRPA is related to the radiative properties of the biomass [29,30]. In our case, MRPA was measured by photonic balance directly in the experiment culture, as represented by Eq. (1) [27]:

$$A = \frac{S}{V C_x} (q_0 - q_L) = \frac{a_s}{C_x} (q_0 - q_L) \quad (1)$$

where  $q_0$  and  $q_L$  refer respectively to the input and output photons flux density (PFD) of the culture in  $\mu\text{mol}_{\text{hv}} \text{ m}^{-2} \text{ s}^{-1}$ .  $C_x$  refers to dry biomass concentration in  $\text{g m}^{-3}$ , and  $a_s$  refers to the specific surface of the PBR in  $\text{m}^{-1}$ , which is the ratio between the illuminated surface  $S$  and the volume of the PBR  $V$ .

### 2.6. Statistical analysis

The statistics were compiled using XLSTAT 2019 software (Addinsoft). After validation of normality with Shapiro-Wilk test and variance homogeneity with Levene test, *t*-test was applied with the use of biological triplicates (each analysis performed 3 times in a row in the same PBR) in experiments presented in Figs. 2 to 6 and 11 to 12, and biological quintuplicate (each analysis performed 5 times in a row in the same PBR) for the results from Figs. 7 to 10.

### 2.7. *Haslea ostrearia* culture

#### 2.7.1. Inoculum

The diatom *Haslea ostrearia* NCC 501 was obtained from MMS laboratory and cultivated in the seawater based Guillard F/2 medium (seawater was provided from the Croisic Loire-Atlantique, France). Cultures of *H. ostrearia* were maintained in 250 mL Erlenmeyer flasks containing 100 mL medium with 10% dilution, after 4–5 days culture in Provasoli ES1/3 (inorganic) modified medium [20] and remodified in total inorganic sources. Light was supplied by white fluorescent light for the day/night cycle 14/10 at  $300 \mu\text{mol m}^{-2} \text{ s}^{-1}$  inside the culture chamber (SANYO MLR-350 culture chamber, Richmond Scientific, UK) at  $16^\circ\text{C}$ . Fresh natural seawater was provided by Le Croisic Océarium

(Loire Atlantique, France) and filtered at 0.7  $\mu\text{m}$  then 0.45  $\mu\text{m}$  before being used for the medium.

### 2.7.2. Immobilized cell PBR

A PBR of 500 mL was designed to culture *H. ostrearia* in immobilized cell conditions. It was designed to limit the shear stress impact of stirring by applying a low liquid recirculation of the medium through the culture (Fig. 1-A). The system was set horizontally, and recirculation of the medium was carried out using a peristaltic pump inducing a low horizontal flowrate of 7  $\text{mL min}^{-1}$  (medium circulation input and output in Fig. 1-A). This value was set semi-empirically to avoid influencing the formation of a biofilm of *H. ostrearia* (data not shown).

Gas was injected through the external wall of the PBR near to the pH probe to better control pH regulation. pH was regulated by  $\text{CO}_2$  injection with an automatized valve. The PFD was provided by setting a horizontal LED panel above the PBR. This prevents any increase in temperature in the culture. The PBR was of Polymethyl methacrylate

(PMMA) material, with a depth of 0.03 m ( $a_s = 33 \text{ m}^{-1}$ ).

This culture system was found to be well-adapted for investigating benthic cell culture, which was obtained by allowing the cells to produce a cell “tissue” naturally at the bottom of the PBR or by creating cell inclusions in agar gel. Agar gel and cell inclusion of *H. ostrearia* was carried out using the Lebeau et al. [14] protocol.

### 2.7.3. Airlift PBR 1 L and 6 L

1 L airlift PBR technology (vertical flat panel) was used to cultivate *H. ostrearia* in conventional mixed conditions. Gas was injected at the center bottom of the PBR, which proved efficient for both mixing and gas-liquid mass transfer. A complete description of this conventional flat panel PBR can be found in literature [18,32].

This technology is more adapted to planktonic (i.e. suspended) cells. It was found that a single localized gas injection was insufficient to prevent cell sedimentation completely, which occurs in the “dead zone” around the gas injection. Regarding shear stress, high values were

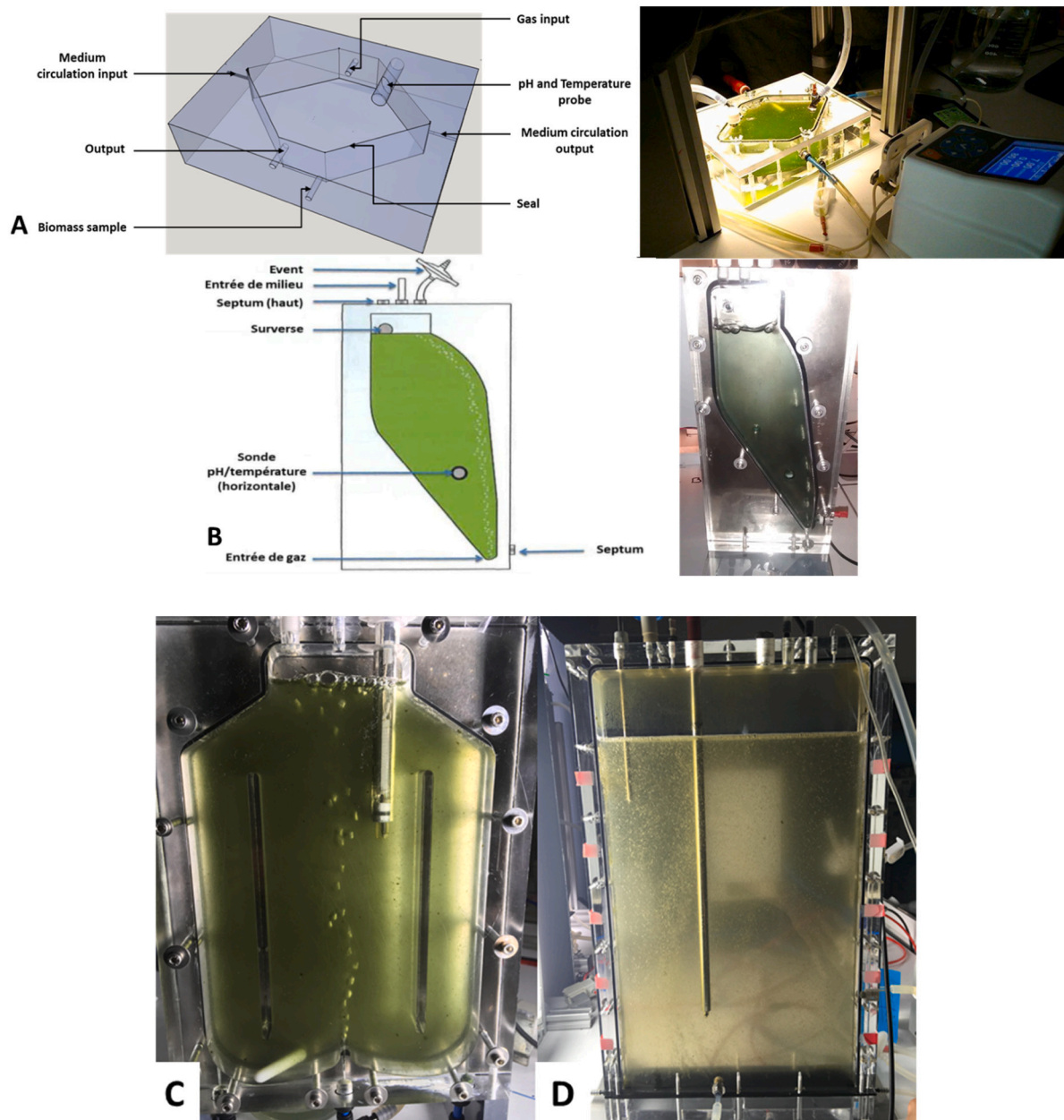


**Fig. 1.** Representation of immobilized cell photobioreactor 500 mL,  $a_s = 33 \text{ m}^{-1}$  (Panel A) of the Crystal photobioreactor 250 mL,  $a_s = 57 \text{ m}^{-1}$  (Panel B), of the airlift 1 L,  $a_s = 33 \text{ m}^{-1}$  (Panel C), and of the airlift 6 L,  $a_s = 33 \text{ m}^{-1}$  (Panel D).

mainly located along the gas path. A value of around  $150 \text{ s}^{-1}$  in this PBR was estimated, with a maximum of  $275 \text{ s}^{-1}$  through the injection axis [32,33]. However, the bubble disruption and coalescence that are present at the top and bottom of the PBR respectively are also known to promote the emergence of micro-vortices capable of producing up to  $14,000 \text{ s}^{-1}$  of mean shear rate [34,35,36].

In addition to the 1 L airlift PBR, a 6 L airlift PBR (vertical flat panel) was used to study the effect of light on *H. ostrearia* culture. This PBR was made of PMMA, which enables determination of the MRPA by measuring PFD  $q_0$  and  $q_L$  on both sides of the PBR (Eq. (1)). The 6 L airlift PBR has a similar design than the 1 L airlift PBR, except that whereas the 1 L airlift PBR had only one gas injection, the 6 L airlift PBR is based on multiple injections by injecting gas through a rubber mat placed on the bottom of the PBR.

This perforated rubber mat allowed a continuous injection of gas along the bottom of the PBR in the form of microbubbles, and consequently homogeneous aeration and stirring of the PBR. The drawback is that the higher values of shear rate obtained in bubble wakes are obtained across almost the entire culture volume, with a higher frequency of bubble disruption/coalescence of microbubbles than in the 1 L PBR [35,37]. Whereas the 1 L airlift PBR does not allow perfect biomass homogeneity, the 6 L airlift PBR provides better cell suspension, which is a mandatory condition for accurate measurement of MRPA in pelagic condition. Note that due to the absence of a dead zone in this PBR, the gas flow rate was reduced every night to avoid the stirring impacting the cell culture during cell division.

#### 2.7.4. Airlift Crystal PBR

The Crystal PBR is an airlift system (vertical flat panel) designed for the culture of microalgae species presenting a high sedimentation rate [38]. Inspired by a settling tank, the shape of this PBR allows cells to settle down to the gas injection, leading to cell re-suspension (Fig. 1-B). This PBR has a culture volume of 250 mL, is 20 mm thick and has an illuminated surface of  $14,426.99 \text{ mm}^2$ . It was used for the first culture test of *H. ostrearia* in mixed conditions.

All the airlift PBRs (1 L, 6 L, Crystal) were controlled at a temperature at  $22 \text{ }^\circ\text{C}$ . This was achieved by regulating the room temperature and with fans at the back of the Crystal PBR only. Light was supplied by LED panels on the day/night cycle 14 h/10 h.

### 3. Results

#### 3.1. Immobilized cell culture

*H. ostrearia* was firstly cultivated in passive cell immobilization used here as a reference protocol for such species, because of its benthic behavior and because effects of shear stress on cells were avoided. The immobilized-cell PBR culture was carried out in continuous mode at dilution rate  $D = 0.1 \text{ d}^{-1}$ ,  $22 \text{ }^\circ\text{C}$  throughout the culture, with pH regulation fixed at 7.8, a PFD of  $200 \mu\text{mol m}^{-2} \text{ s}^{-1}$  in the day/night cycle 14/10 and cultivated in ES1/3 (inorganic) modified medium. As a passive cell immobilization culture, the biomass was not mixed and allowed to fix naturally at the bottom of the PBR. It was compared with the agar cell inclusion culture (i.e. active immobilization), which was conducted in the same PBR under the same conditions. The cellular concentration included in agar gel was adjusted to achieve similar cell density to the passive-cell immobilized culture inoculation. Note that cell immobilization in alginate beads was also carried out but no positive results were obtained (data not shown).

Time evolutions of cell density, EMn and dissolved organic concentrations are given in Fig. 2. For biomass concentration, only values at  $t_0$  ( $4.13 \times 10^7 \text{ cell L}^{-1}$  for passive;  $4.18 \times 10^7 \text{ cell L}^{-1}$  for active culture) and  $t_{\text{end}}$  (cell death) were carried out.

Regarding immobilization, cell death was observed at day 9 whatever the passive or active culture. Immobilized cell culture being demonstrated elsewhere, this could be attributed to our growing conditions (see below). Our experiments, however, were found to be sufficient for estimating marennine production. Both culture techniques revealed maximum production at day 4, with  $3.7 \pm 0.34 \text{ mg}_{\text{EMn}} \text{ L}^{-1}$  and  $4.5 \pm 0.34 \text{ mg}_{\text{EMn}} \text{ L}^{-1}$  for active immobilized and passive immobilized cultures respectively. In either case, EMn production over time was found to be unstable and led to a progressive decrease in EMn concentration, doubtless due to cell death.

The loss of culture under these conditions of immobilized cells was obtained despite several attempts. This could not be attributed to shear stress, and the culture medium was validated elsewhere (see below). One explanation could be the DIC concentration, as shown in Fig. 2. Values given here are an average of the concentrations obtained in passive and active cell immobilization tests, as similar values were achieved. A progressive decrease was obtained, which could lead to the

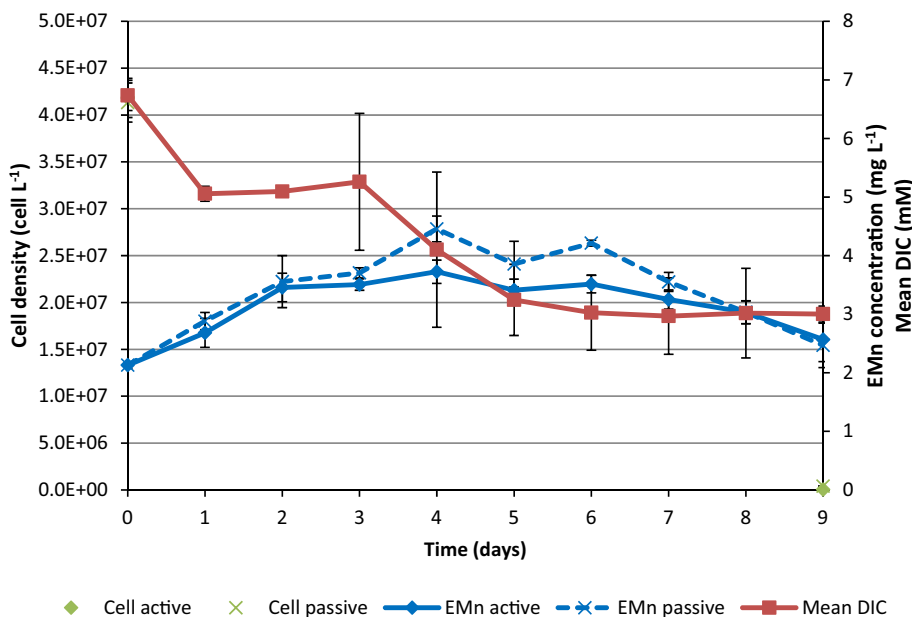


Fig. 2. Continuous culture of *Haslea ostrearia* in immobilized cell PBR, with passive (natural cells attachment to the bottom of the PBR) and active (agar cell inclusion) immobilization. Data is mean  $\pm$  SD ( $n = 3$  and  $n = 2$  for mean DIC).

appearance of carbon limitation. It is known that immobilization reduces mass transfer in the cell's biofilm. Since a decrease in DIC contributes to the decrease of this mass transfer, it could lead to limitation of the cells' access to the carbon source in the film, leading to cell death. Because the immobilization approach was only applied to obtain some preliminary values in EMn production for future comparisons to other culture techniques, this was not investigated further. The effect of carbon supply was investigated in suspended cell conditions (see section below).

### 3.2. *Haslea ostrearia* culture in Crystal PBR

#### 3.2.1. Investigation of CO<sub>2</sub> tolerance of *Haslea ostrearia* in batch culture

CO<sub>2</sub> intolerance in *H. ostrearia* was hypothesized by Robert [20]. In a natural environment, *H. ostrearia* usually grows on the bottom of a biofilm, and consequently has natural protection against the gas phase. As increasing the CO<sub>2</sub> content in the gas phase increases dissolved inorganic carbon concentration in the liquid phase, two air enrichments of CO<sub>2</sub> (2 and 15%) were tested in suspended cell culture. The pH value was kept constant and similar for the two experiments, to avoid from a possible bias due culture medium acidification generated by the increase of CO<sub>2</sub> dissolution [39]. Two air enrichments of CO<sub>2</sub> (2 and 15%) were tested in suspended cell culture. A Crystal PBR was used because of its efficiency with cells presenting a high sedimentation rate. Batch cultures with the same conditions as for immobilized cell culture were conducted

(22 °C, pH regulation fixed at 7.8) with an incident PFD of 115 μmol<sub>hv</sub> m<sup>-2</sup> s<sup>-1</sup> in day/night cycle 14/10. The incident PFD was modified to take into account the larger specific illuminated surface of the Crystal PBR (i.e. lower depth of culture). Results are given in Fig. 3.

A marked effect of the CO<sub>2</sub> supply was observed. Cell densities reached 2.5 × 10<sup>8</sup> cell L<sup>-1</sup> at day 8 and 1.4 × 10<sup>8</sup> cell L<sup>-1</sup> at day 6 for 15% CO<sub>2</sub> and 2% CO<sub>2</sub> respectively (*t*-test *p* < 0.001). The main impact was on EMn production, which reached 7.3 mg L<sup>-1</sup> against 1.0 mg L<sup>-1</sup> with 15% CO<sub>2</sub> and 2% CO<sub>2</sub> at day 10 respectively (*t*-test *p* < 0.001). We noted a decrease in EMn concentration for the 2% CO<sub>2</sub>. This could be attributable to EMn degradation or consumption by bacteria. Finally, *H. ostrearia* was found to tolerate CO<sub>2</sub>-enriched gas injection when combined with pH regulation. Increasing the proportion of CO<sub>2</sub> (and consequently the carbon transferred to the gas phase, as shown in next section) revealed an increase in both cell density and EMn concentration. The relevance of carbon limitation on *H. ostrearia* culture was therefore confirmed.

#### 3.2.2. Assessment of *Haslea ostrearia* growth in continuous mixed culture

To assess the possibility of cultivating *H. ostrearia* in suspended cells conditions, a continuous culture was conducted under mixed conditions in a Crystal PBR (i.e. airlift PBR). The CO<sub>2</sub> supply in the gas phase was set at 15% and the same conditions as in previous batch culture were applied. The dilution rate was set at *D* = 0.1 d<sup>-1</sup>. Results are given in Fig. 4.

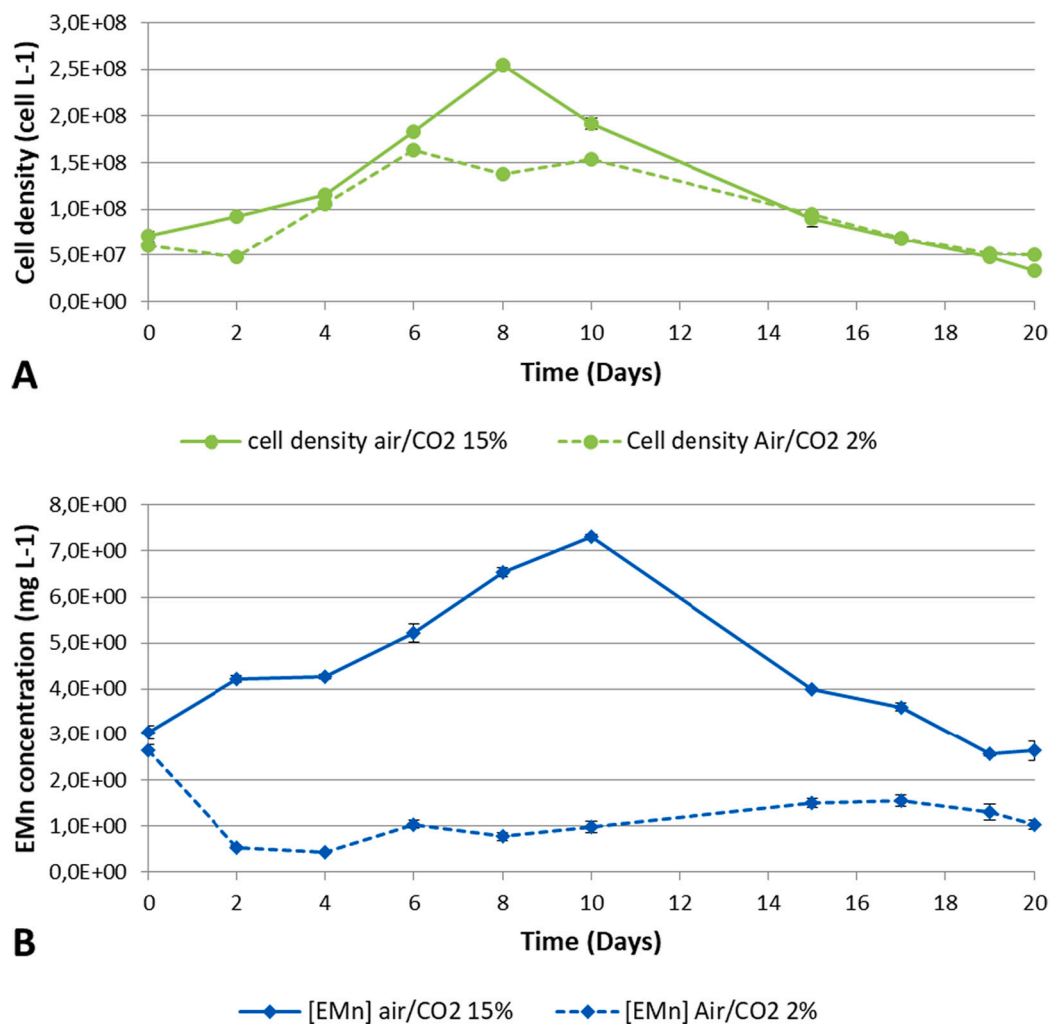


Fig. 3. Batch culture of *Haslea ostrearia* for 2% and 15% air/CO<sub>2</sub> proportion for cell density (A) and extracellular marennine concentration (EMn) (B), in Crystal PBR. Data is mean ± SD (n = 3).

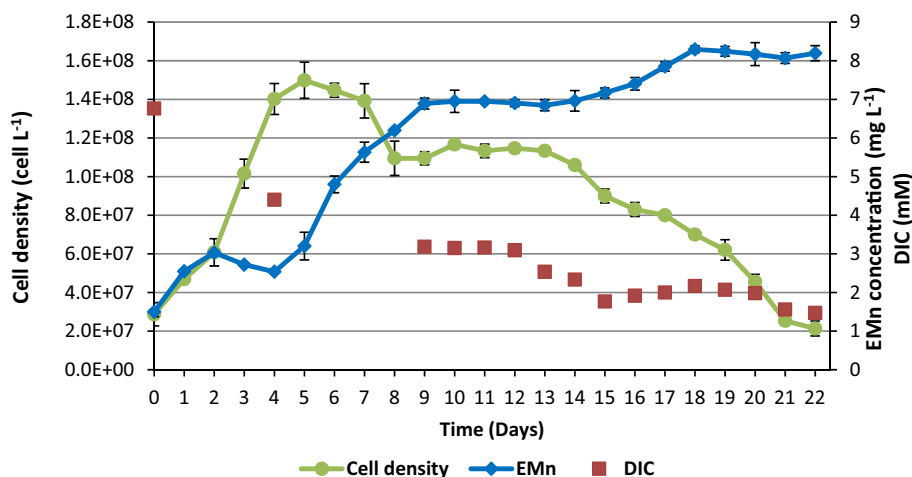


Fig. 4. Continuous culture of *Haslea ostrearia* at 15% CO<sub>2</sub> in a Crystal PBR. Cell density, extracellular marennine (EMn) and dissolved inorganic carbon (DIC) were measured. Data is mean ± SD (n = 3).

A maximum cell density of  $1.5 \pm 0.1 \times 10^8$  cell L<sup>-1</sup> was reached at day 5 before decreasing to  $1.1 \pm 0.04 \times 10^8$  cell L<sup>-1</sup> at day 9. Regarding EMn production, the stirred continuous culture led to a productivity of  $6.9 \pm 0.1$  mg<sub>EMn</sub> L<sup>-1</sup> at day 9 and  $8.2 \pm 0.2$  mg<sub>EMn</sub> L<sup>-1</sup> at day 22. These values can be compared to immobilized-cell continuous culture which reached a maximum of  $4.5 \pm 0.3$  mg<sub>EMn</sub> L<sup>-1</sup>. The interest of cultivating *H. ostrearia* in mixed conditions was here confirmed.

We can note also that both cell density and EMn concentration, as well as inorganic carbon concentration, stabilized at day 8 for 4 days, before a decrease in cell density and inorganic carbon. EMn concentration then started to increase (day 15), demonstrating EMn synthesis or intracellular marennine (IMn) release in the medium. Despite the 15% CO<sub>2</sub> injection, dissolved inorganic carbon was also found to decrease continuously, as observed previously in the immobilized cell PBR culture. This indicated the need for a further increase in carbon supply to avoid possible growth limitation.

### 3.3. Investigation of nutrient consumption in PBR culture

#### 3.3.1. Carbon consumption

Carbon availability in the liquid phase can limit growth [40,41]. The DIC concentration was then raised by adding sodium bicarbonate at the beginning of the culture. Le Gouic [39] estimated that *Chlorella vulgaris* needs up to 10 mM of DIC to avoid carbon limitation, which could be given either by a phase of gas injection enriched with CO<sub>2</sub>, or by dissolution of a chemical carbon source in the medium. 10 mM corresponds to a sodium bicarbonate concentration of 1.2 g L<sup>-1</sup>. This concentration was found to lead to nutrient precipitation in the seawater-based medium due to the interaction of silicon, phosphate and carbonate with Ca<sup>2+</sup> and Mg<sup>2+</sup> endogenous entities in seawater [42,43].

*H. ostrearia* was therefore cultivated in semi-continuous mode in the 1 L airlift PBR, with a fed-batch strategy conducted on a sodium bicarbonate source. For this purpose, a solution of sodium bicarbonate (5 mM maximum) was injected punctually every day. Because of the parallel CO<sub>2</sub> injection, this enabled us to raise the final DIC to around 10 mM while avoiding the precipitation phenomenon. This was added to the ES1/3 medium (6N24P inorganic medium), which was optimized for *H. ostrearia* growth in PBR [17]. The semi-continuous mode was selected to cultivate *H. ostrearia* because of its benthic characteristic, which leads to an inhomogeneous culture. Harvesting was then applied for a limited period of time per day. Other parameters were similar: temperature was fixed at 22 °C throughout the culture, pH regulation was fixed at 7.8 and PFD at 200 μmol m<sup>-2</sup> s<sup>-1</sup> (measured to obtain the same MRPA value according to the different a<sub>s</sub> of the PBRs, see Eq. (1)) in day/night cycle 14/10 and dilution rate at D = 0.1 d<sup>-1</sup> (Fig. 5).

Unlike with previous experiments, a constant production of biomass and EMn was obtained throughout the semi-continuous culture. Dry biomass concentration reached 320 mg<sub>X</sub> L<sup>-1</sup>, corresponding to  $2.6 \times 10^8$  cell L<sup>-1</sup> and an EMn concentration of up to 8.2 mg<sub>EMn</sub> L<sup>-1</sup>. DIC concentration was found to stabilize progressively at the targeted 10 mM concentration. The carbon-fed batch strategy was therefore found to be suitable to obtain a stable and constant productivity of  $31.7 \pm 0.5$  mg<sub>X</sub> L<sup>-1</sup> d<sup>-1</sup> of biomass and  $0.8 \pm 0.2$  mg<sub>EMn</sub> L<sup>-1</sup> d<sup>-1</sup>.

#### 3.3.2. Silicon, nitrogen and phosphorus consumption

Silicon and phosphorus consumption was investigated during the semi-continuous culture (data not shown). All nutrients were found to decrease, as expected. Nitrate decreased to 57% of its initial concentration (1.73 mM) but without deprivation, with a final concentration of around 1 mM. Phosphate and silicon dioxide concentrations showed a marked decrease and could therefore be suspected of limiting cell growth (around 0.7% of the initial concentration after 4 days). Time evolutions of the main nutrients enabled us to determine the substrate consumption rates (r<sub>s</sub>), specific substrate consumption rates (Q<sub>s</sub>) and yield factor (Y<sub>X</sub>) for NO<sub>3</sub><sup>-</sup>, PO<sub>4</sub><sup>-</sup> and SiO<sub>3</sub><sup>2-</sup> (Table 1, see also [18] for calculation details).

PO<sub>4</sub><sup>2-</sup> and SiO<sub>3</sub><sup>2-</sup> consumption rates were found to be respectively  $1.0 \times 10^{-1}$  and  $9.2 \times 10^{-2}$  μmol L<sup>-1</sup> d<sup>-1</sup>; 3 times less than the NO<sub>3</sub><sup>-</sup> consumption rate. The specific substrate consumption rate enables us to determine the need for these nutrients. The values obtained here emphasize the need to increase SiO<sub>3</sub><sup>2-</sup> and PO<sub>4</sub><sup>2-</sup> concentration in the ES 1/3 medium to avoid any limitation. However, SiO<sub>3</sub><sup>2-</sup> and PO<sub>4</sub><sup>2-</sup> are highly precipitating molecules with Ca<sup>2+</sup> and Mg<sup>2+</sup> ions, such as sodium bicarbonate [38,41]. It was therefore decided to extend the fed-batch strategy on HCO<sub>3</sub><sup>-</sup> to PO<sub>4</sub><sup>2-</sup>, SiO<sub>3</sub><sup>2-</sup>. The nutrient feeding rate was based on the specific substrate consumption rate (Table 1) to ensure no limitation of the nutrient and that no precipitation phenomenon would occur. For a productivity of P<sub>V</sub> = 28.33 mg<sub>X</sub> L<sup>-1</sup> d<sup>-1</sup>, *H. ostrearia* would need, for example, a fed-batch of  $1.1 \times 10^{-2}$  μmol L<sup>-1</sup> d<sup>-1</sup> of SiO<sub>3</sub><sup>2-</sup> nutrient and  $1.2 \times 10^{-2}$  μmol L<sup>-1</sup> d<sup>-1</sup> for PO<sub>4</sub><sup>2-</sup>. This fed-batch strategy was implemented in a semi-continuous culture on ES 1/3 medium (6N24P inorganic). No further increase in either biomass or EMn productivity was observed (data not shown). Thus, a further increase in N and P concentrations was applied, and *H. ostrearia* was cultivated on 12N48P. The temperature was fixed at 22 °C throughout the culture, pH regulation was fixed at 7.8, the PFD at 330 μmol m<sup>-2</sup> s<sup>-1</sup> in day/night cycle 14/10 and the dilution rate at D = 0.1 d<sup>-1</sup>. Results are given in Fig. 6.

The fed-batch strategy applied to P-C-Si elements was found to prevent any precipitation phenomenon in semi-continuous mode culture.

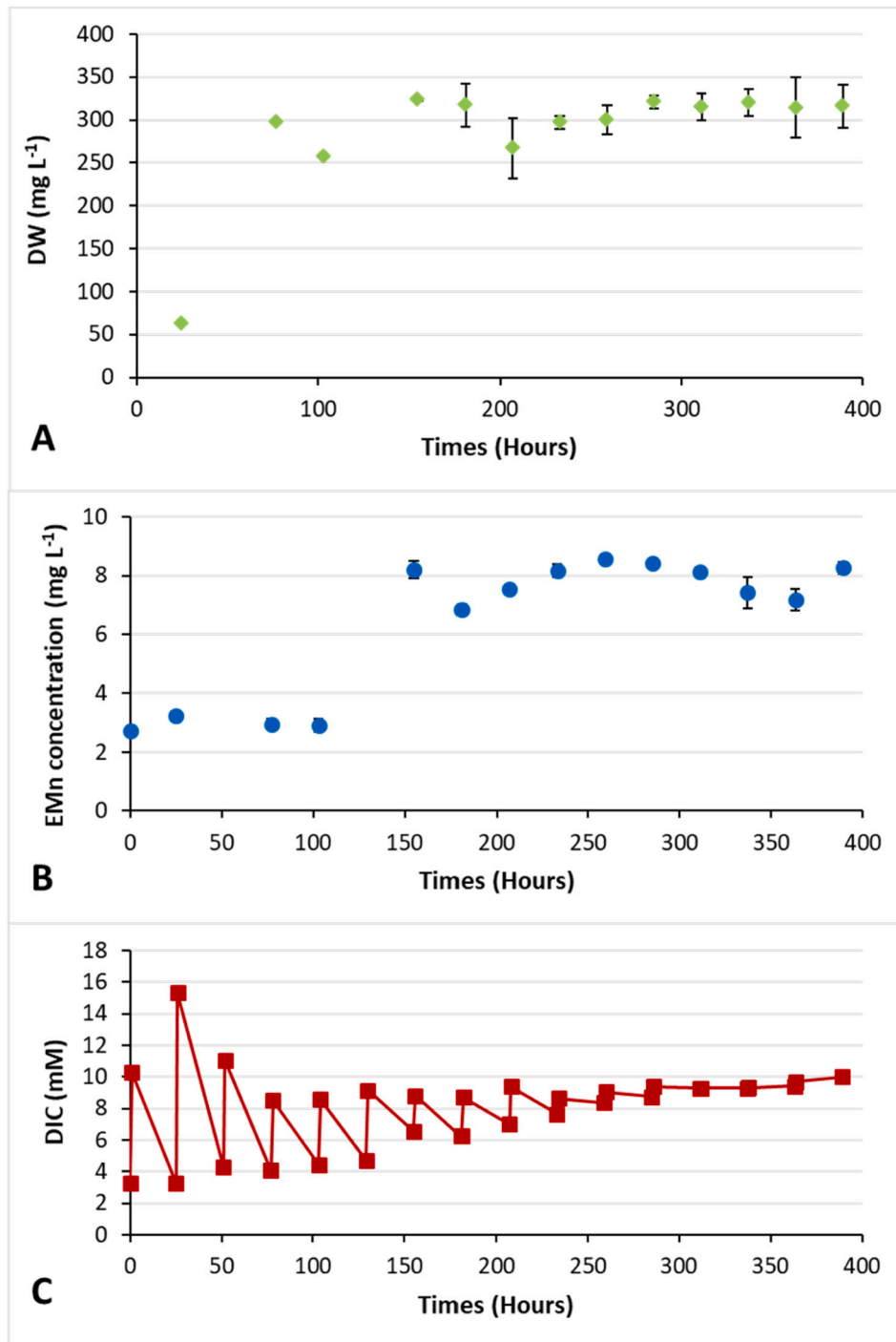


**Fig. 5.** Semi-continuous culture of *Haslea ostrearia* in 1 L airlift PBR with carbon fed-batch and 2% CO<sub>2</sub>. Dry weight (DW), extracellular marennine concentration (EMn) and dissolved inorganic carbon (DIC) were measured. Data is mean ± SD (n = 3).

**Table 1**

Nutrient consumption of *Haslea ostrearia* ( $r_s$ ,  $Q_s$  and  $Y_x$  determination for NO<sub>3</sub><sup>-</sup>, PO<sub>4</sub><sup>2-</sup> and SiO<sub>2</sub><sup>2-</sup>) in semi-continuous culture in an airlift PBR.

	NO <sub>3</sub> <sup>-</sup>	PO <sub>4</sub> <sup>2-</sup>	SiO <sub>2</sub> <sup>2-</sup>
$r_s$ (μmol L <sup>-1</sup> d <sup>-1</sup> )	$3.0 \times 10^{-1}$	$1.0 \times 10^{-1}$	$9.2 \times 10^{-2}$
$Q_s$ (μmol g <sub>x</sub> <sup>-1</sup> d <sup>-1</sup> )	1.3	$4.3 \times 10^{-1}$	$3.9 \times 10^{-1}$
$Y_x$ (μmol g <sub>x</sub> <sup>-1</sup> )	$9.4 \times 10^{-3}$	$3.2 \times 10^{-3}$	$2.9 \times 10^{-3}$

This allowed the provision of macronutrients such as N, P, Si and C in higher concentrations, leading to a 12N48P medium.

A constant biomass and EMn production were obtained, stable over a period of more than 20 days. However, whereas biomass productivity reached  $51.8 \pm 3.9 \text{ mg}_x \text{ L}^{-1} \text{ d}^{-1}$ , EMn productivity only reached  $0.2 \pm 0.2 \text{ mg}_{\text{EMn}} \text{ L}^{-1} \text{ d}^{-1}$ . Medium enrichment in Si and P could therefore have a negative impact on EMn synthesis, reducing EMn productivity from  $0.8 \pm 0.2 \text{ mg}_{\text{EMn}} \text{ L}^{-1} \text{ d}^{-1}$  (Fig. 5 B) to  $0.2 \pm 0.1 \text{ mg}_{\text{EMn}} \text{ L}^{-1} \text{ d}^{-1}$ . On the other hand, it significantly increased biomass concentration, up to  $522 \text{ mg}_x \text{ L}^{-1}$  (equal to  $4.22 \times 10^8 \text{ cell L}^{-1}$ ). This value can be considered high compared to *H. ostrearia* standards. Additionally, stable production such

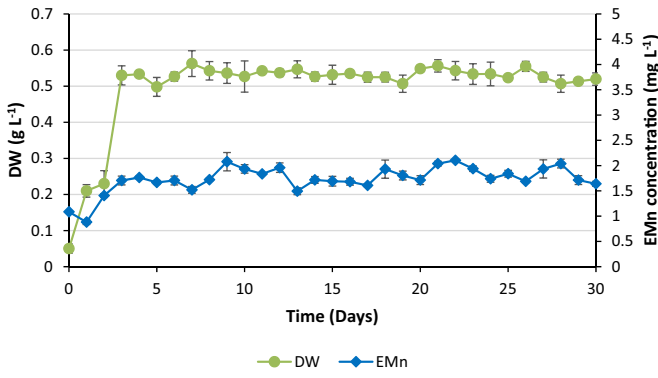


**Fig. 6.** Semi-continuous *Haslea ostrearia* cell culture in 1 L airlift PBR with C, P, Si fed-batch conditions. Dry weight (DW) and extracellular marennine concentration (EMn) were measured. Data is mean  $\pm$  SD (n = 3).

as this can be considered an important methodologic achievement. This opens up the possibility of further optimization of *H. ostrearia* culture in suspended cells. The section below presents the investigation of light tolerance in a 6 L airlift PBR.

### 3.4. The ingathering of optimal growth parameters for biomass and EMn production

#### 3.4.1. Light tolerance and cell response

This study was carried out in the 6 L airlift PBR, in order to measure input and output PFD for MRPA measurement (Eq. (1)). For PBR of flat panel type with fully transparent walls as used in this study, those PFD are directly obtained from the front (i.e. illuminated) and back side of the PBR. The temperature of the culture was fixed at 22 °C, pH regulation at 7.8 and dilution rate at  $D = 0.1 \text{ d}^{-1}$ . The test was carried out with 6 different PFDs ranging from 140 to 400  $\mu\text{mol m}^{-2} \text{ s}^{-1}$  (140, 165, 210, 300, 350, 400  $\mu\text{mol m}^{-2} \text{ s}^{-1}$ ), with a day/night cycle 14 h/10 h. Each culture was monitored for 3 times the residence time to obtain a constant productivity (Fig. 7).

The results given in Fig. 7-A reveal that both EMn and biomass were found to be closely related to MRPA values. This indicates a light tolerance of the cell response in both growth (as it should be) and also EMn production. An optimal MRPA value was achieved for both, indicating a light tolerance of biological responses. Concerning biomass productivity, the highest values were achieved in the range 10.7–12.3  $\mu\text{mol}_{\text{hv}} \text{ g}_x^{-1} \text{ s}^{-1}$ , leading respectively to  $1.6 \pm 0.2$  and  $1.7 \pm 0.2 \text{ g}_x \text{ m}^{-2} \text{ d}^{-1}$ . However, the highest EMn productivity was  $11.0 \pm 0.6 \text{ mg}_{\text{EMn}} \text{ m}^{-2} \text{ d}^{-1}$  which was obtained at  $8.4 \mu\text{mol}_{\text{hv}} \text{ g}_x^{-1} \text{ s}^{-1}$ , with a different optimal value, therefore, than for biomass growth. With both biomass and EMn, MRPA higher and lower than  $12.3 \mu\text{mol}_{\text{hv}} \text{ g}_x^{-1} \text{ s}^{-1}$  resulted in lower productivity. We can also note that the range of optimal MRPA values, as well as the profile of the curves achieved, are close to the photosynthetic growth response of *Chlorella vulgaris* and *Nannochloropsis gaditana* [44].

The results can be combined to determine light conversion efficiency, which represents the amount of biomass produced per  $\mu\text{mol}_{\text{hv}}$  absorbed ( $\text{g}_x \text{ mol}_{\text{hv}}^{-1}$ ):

$$\eta_{x/\text{hv}} = \frac{S_x}{(q_0 - q_L)} \quad (2)$$

where  $S_x$  represent the surface productivity in  $\text{g m}^{-2} \text{ d}^{-1}$ .

Fig. 7-B presents the results of light conversion efficiency and total pigment content. Both evolutions as a function of the MRPA are found to be similar here. Light conversion efficiency was found to decrease for values lower than 6 and higher than  $14 \mu\text{mol}_{\text{hv}} \text{ g}_x^{-1} \text{ s}^{-1}$ , with maximal values around  $0.10 \pm 0.01 \text{ g}_x \text{ mol}_{\text{hv}}^{-1}$  in the range 8 and  $12 \mu\text{mol}_{\text{hv}} \text{ g}_x^{-1} \text{ s}^{-1}$ .

The highest pigmentation result ( $2.9 \pm 0.1\% \text{ w/w}$ ) was found at  $12.3$

$\mu\text{mol}_{\text{hv}} \text{ g}_x^{-1} \text{ s}^{-1}$ , a value similar to the optimal MRPA condition for biomass productivity. We can note that the reverse would be expected, with a progressive decrease in pigment content with increasing MRPA value as a result of the well-known pigment acclimation process (i.e. decrease of pigment content with increased light absorption). This could be attributed to the effect of marennine. In fact, the EMn content, which is also presented in Fig. 7-B, decreases continuously with the rise in MRPA, with a decrease in EMn (%) from  $1.89 \pm 0.08\%$  to  $0.17 \pm 0.05\%$ . We can note that the EMn content curves cross the total pigment curve at  $8 \mu\text{mol}_{\text{hv}} \text{ g}_x^{-1} \text{ s}^{-1}$ , corresponding also to maximal light conversion efficiency of biomass for *H. ostrearia*. As an additional value of interest to better understand EMn excretion as a function of light, the light conversion efficiency into EMn was added (Fig. 7-C). The decrease of light conversion into EMn occurs for values larger than  $8 \mu\text{mol}_{\text{hv}} \text{ g}_x^{-1} \text{ s}^{-1}$ , which also leads to an increase in light conversion into biomass efficiency (Fig. 7-B). Those results tend then to emphasize that a MRPA value of  $8 \mu\text{mol}_{\text{hv}} \text{ g}_x^{-1} \text{ s}^{-1}$  triggers lower EMn production in favor of biomass. The EMn content, which is also presented Fig. 7-B, decreases continuously with the rise in MRPA. However, the EMn content curves appear to cross the total pigment curve at  $8 \mu\text{mol}_{\text{hv}} \text{ g}_x^{-1} \text{ s}^{-1}$ , representing a maximal light conversion efficiency of biomass for *H. ostrearia*.

To better understand EMn excretion as a function of light, the light conversion efficiency of EMn was added (Fig. 7-B). As well as total photosynthetic pigment content correlated to light conversion into biomass efficiency, a similar evolution for the EMn produced (% w/w) and light conversion into EMn efficiency was obtained. The rise in MRPA leads to a decrease in EMn (%) from  $1.89 \pm 0.08\%$  to  $0.17 \pm 0.05\%$ . The decrease in light conversion into EMn efficiency occurs at  $8 \mu\text{mol}_{\text{hv}} \text{ g}_x^{-1} \text{ s}^{-1}$ , which also leads to an increase in light conversion into biomass efficiency. Those results show that  $8 \mu\text{mol}_{\text{hv}} \text{ g}_x^{-1} \text{ s}^{-1}$  triggers lower EMn production in favor of biomass.

#### 3.4.2. pH and temperature optimization

The goal of this experiment was to observe and measure the impact of pH and temperature conditions on *H. ostrearia* culture in order to select the optimal values ( $T_{\text{opt}}$  and  $\text{pH}_{\text{opt}}$ ) for EMn production. The culture was carried out in a 1 L airlift PBR in semi-continuous mode using a P, Si, C fed-batch strategy. For pH value optimization, the temperature of the culture was firstly fixed at 22 °C throughout, the dilution rate at  $D = 0.1 \text{ d}^{-1}$  and pH regulation was fixed at 6; 7.8; 8.3; 9. The PFD was fixed at  $300 \mu\text{mol m}^{-2} \text{ s}^{-1}$  (to obtain an optimal value of MRPA  $A_{\text{opt}}$  around  $12 \mu\text{mol}_{\text{hv}} \text{ g}_x^{-1} \text{ s}^{-1}$  as determined in previous section) in the day/night cycle 14/10. All cultures were monitored for 3 times the residence time to achieve constant biomass productivity. Results are given in Fig. 8-A (the presence of the \* symbol indicates the presence of visual chemical precipitation throughout the culture).

Optimum surface biomass productivity ( $1.63 \pm 0.04 \text{ g}_x \text{ m}^{-2} \text{ d}^{-1}$ ) and maximum concentration in total pigment ( $2.42 \pm 0.07\%$ ) were obtained at pH 8.3. However, for the same pH EMn productivity was low, reaching only  $5.27 \pm 0.21 \text{ mg}_{\text{EMn}} \text{ m}^{-2} \text{ d}^{-1}$ . pH 6 also showed low EMn productivity, biomass and pigment concentration respectively at  $6.71 \pm 0.33 \text{ mg}_{\text{EMn}} \text{ m}^{-2} \text{ d}^{-1}$ ,  $0.63 \pm 0.05 \text{ g}_x \text{ m}^{-2} \text{ d}^{-1}$  and  $0.48 \pm 0.05\%$ . However, pH 7.8 led to interesting EMn results with  $14.10 \pm 0.56 \text{ mg}_{\text{EMn}} \text{ m}^{-2} \text{ d}^{-1}$ ; the best results for this study.

Pigment content was found to follow the same evolution as for biomass productivity, which tends to attest to the direct relation of pH to *H. ostrearia* photosynthetic growth. However, the results should be considered in hindsight because of the consequences of pH variation. pH value is known to greatly impact the medium chemistry of *H. ostrearia*, which could induce a limiting of nutrient conditions due to precipitation or chemistry interaction with EMn. This hypothesis is supported by the increasing precipitation with increasing pH value. pH 9 was found to lead to a high level of precipitation, which raises the chemistry instability of the medium [17]. Despite this precipitation, pigment concentration was found to be higher at pH 8.3 with  $2.42 \pm 0.08\%$  than for pH 7.8. Finally, this raises the possibility of a  $\text{pH}_{\text{opt}}$  close to 8.3 while

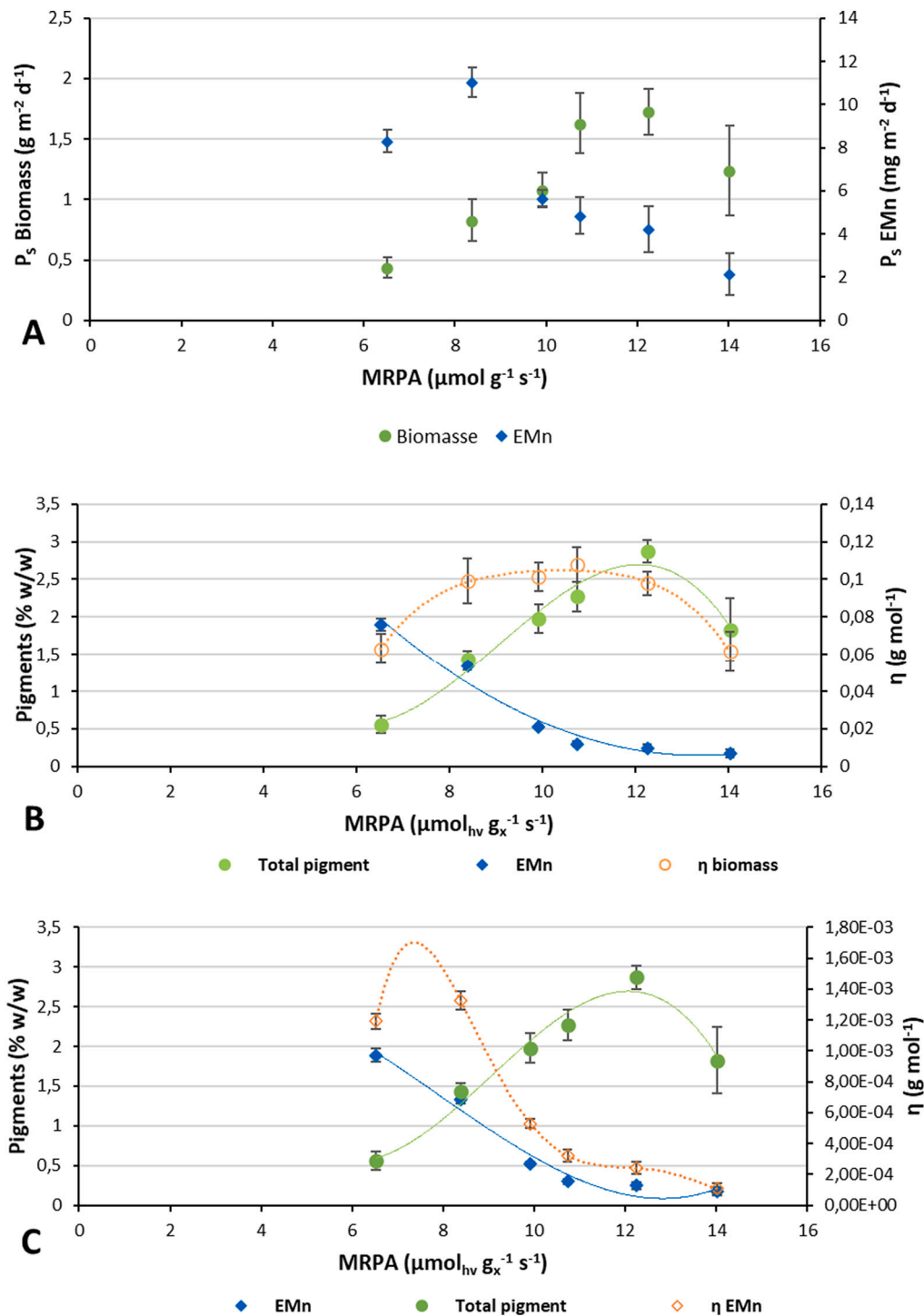


**Fig. 7.** Light tolerance curves of *Haslea ostrearia*. Panel A describes the evolution of surface productivity ( $P_s$ ) depending on MRPA values for biomass and extracellular marennine (EMn) results. Total pigment and extracellular marennine (EMn) are given in Panels B and C. as a function of MRPA, as well as the light conversion efficiency ( $\eta$ ) into biomass (Panel B) and into EMn (Panel C). Data is mean  $\pm$  SD ( $n = 5$ ).

avoiding any high level of precipitation.

Although the best biomass and pigment productivity result was achieved at pH 8.3, the best EMn productivity was achieved at pH 7.8, which also exhibits no visual precipitation. Because the culture of *H. ostrearia* was found to be more convenient at pH 7.8 due to the precipitation phenomenon being amplified in higher pH conditions, the pH value of 7.8 was selected as  $\text{pH}_{\text{OPT}}$  for the rest of the studies.

In a second series of experiments, the impact of temperature conditions on *H. ostrearia* culture was investigated in order to select the

optimal temperature ( $T_{\text{OPT}}$ ) condition for EMn production. Same conditions as in the experiments for pH value optimization were applied, except temperature which was regulated at 16; 22; 25; 30 °C throughout, and pH regulation which was fixed at 7.8. The results are given in Fig. 8-B.

Temperature was found to impact the *H. ostrearia* culture, but mainly by triggering the precipitation phenomenon which could negatively impact cell culture, as presented above for the pH study. Precipitation was found to occur at temperatures higher than 22 °C. Considering only

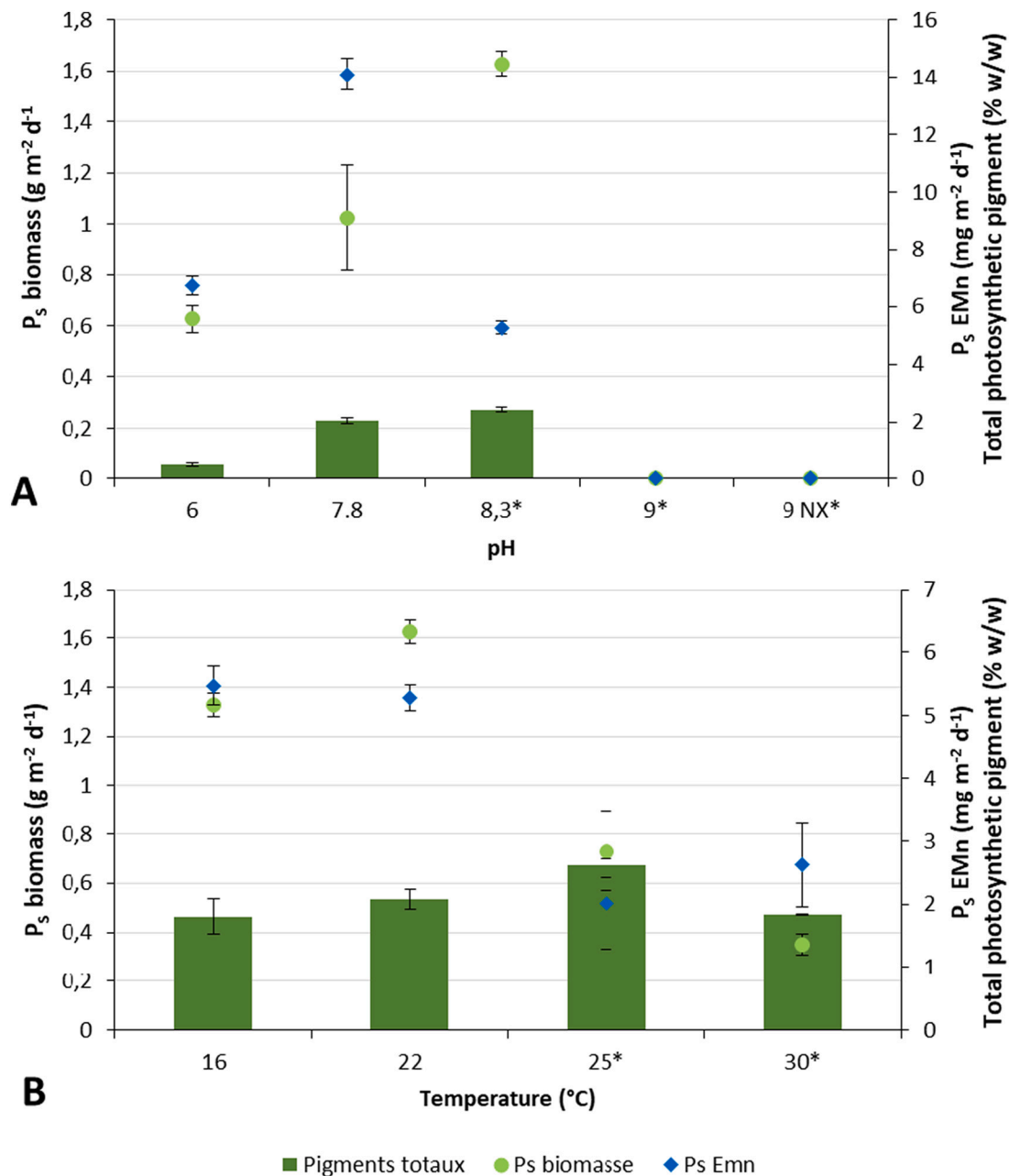


**Fig. 8.** pH (Panel A) and temperature (Panel B) effects on *Haslea ostrearia* total photosynthetic pigment concentration, biomass and extracellular marennine (EMn) productivities ( $P_s$ ) in semi-continuous culture in 1 L airlift PBR. The presence of the \* symbol indicates the presence of visual precipitation throughout the culture. Data is mean  $\pm$  SD (n = 5).

a non-precipitate culture initially, the highest biomass results were achieved at 22 °C with  $1.63 \pm 0.05 \text{ g}_x \text{ m}^{-2} \text{ d}^{-1}$ . There was therefore no significant impact ( $t$ -test  $p = 0.748$  for  $n = 5$ ) of temperature on EMn productivity between 16 and 22 °C. In terms of pigment concentration, there was no significant impact ( $t$ -test  $p = 0.563$  for  $n = 5$ ) at 16 °C with  $1.80 \pm 0.27\%$  compared to 22 °C culture with  $2.08 \pm 0.15\%$ , but a higher pigment concentration is reached at 25 °C with  $2.62 \pm 0.19\%$ .

As with the pH study, the precipitation phenomenon definitely impacts biomass and EMn. It can be noted, however, that pigment concentration is higher at 25 °C even though precipitation occurs. These results raise the possibility of a  $T_{OPT} = 25 \text{ °C}$ , however, precipitation also impacts biomass productivity greatly, decreasing it from  $1.63 \pm 0.05 \text{ g}_x \text{ m}^{-2} \text{ d}^{-1}$  to  $0.73 \pm 0.16 \text{ g}_x \text{ m}^{-2} \text{ d}^{-1}$  in the 25 °C and 30 °C experiment. EMn productivity also decreased with the increase in temperature. There could be various explanations for this: the molecule could be

degraded at a higher temperature, less could be produced by the cell or it could interact with the precipitation phenomenon. Finally, because of the precipitation phenomenon, 22 °C was considered as  $T_{OPT}$  for the rest of the study.

#### 3.4.3. Physiologic stress for EMn overproduction

Based on previous results, the optimal values for MRPA, temperature and pH were gathered ( $A_{OPT}$ ,  $T_{OPT}$  and  $pH_{OPT}$ ) for *H. ostrearia* culture. Different conditions were then tested to induce stressing conditions for EMn overproduction. Fig. 6 shows continuous production of EMn in a semi-continuous culture without nutrient limitation. This was retained as a reference. Even in unrestricted conditions, the productivity of EMn was found to be low at  $0.2 \text{ mg}_{EMn} \text{ L}^{-1} \text{ d}^{-1}$ , corresponding to  $6.06 \text{ mg}_{EMn} \text{ m}^{-2} \text{ d}^{-1}$ .

The following experiment consists of measuring EMn, biomass, cell

and pigment productivity in order to understand if nutrient depletion or limitation leads to overproduction of EMn. This was investigated for nitrogen, phosphorus, silica and carbon nutrient. This study was carried out in a 1 L airlift PBR and under the same culture conditions as previously, but with  $T_{OPT} = 22\text{ }^{\circ}\text{C}$ ,  $pH_{OPT} = 7.8$  and  $A_{OPT} = 12.3\text{ }\mu\text{mol}_{hv}\text{ g}_x^{-1}\text{ s}^{-1}$ . Once a sufficient biomass was obtained in nutrient replete conditions, the feeding medium and around 75% of the culture volume in the PBR were replaced by the limited or deprived culture medium. The mixing was previously stopped to let cells sediment and to avoid removing too much cells. Depletion conditions were obtained by applying a nutrient-free medium, which was previously prepared by simply recovering the nutrient of interest from the medium composition. Nutrient concentration for limitation conditions was fixed with regard to the 20-times diluted culture of Rossignol [13]. These concentrations represent  $2.39 \times 10^{-4}\text{ M}$  for nitrogen,  $3.05 \times 10^{-5}\text{ M}$  for phosphorus and  $5.49 \times 10^{-5}\text{ M}$  for silica. All cultures were monitored for 3 times the residence time to confirm constant productivity (Fig. 9).

The impact of nutrient limitation and depletion on pigment concentration can be observed in Fig. 9. None of the depleted or limited culture offers any increase in pigment concentration, with values below  $2.5 \pm 0.2\%$ . *H. ostrearia* pigment synthesis is highly reduced by nitrogen depletion and limitation, at  $0.7 \pm 0.3\%$  and  $1.2 \pm 0.4\%$  respectively. Both results can be explained by the high nitrogen requirement for protein synthesis. The reduction of pigment content shows the cell's capacity to adapt to balance its composition in order to survive, and certainly impacts the cell's photosynthetic efficiency.

The results are therefore analyzed in terms of EMn and biomass productivity (Fig. 10). Depletion and limitation were found to reduce biomass productivity by almost 2.7 times compared to the unrestricted culture. In terms of EMn productivity, depletion conditions only led to lower productivity than the unrestricted culture, at  $5.3 \pm 0.2\text{ mg}_{EMn}\text{ m}^{-2}\text{ d}^{-1}$ . However, P, Si and N limitation conditions led to higher productivity,  $9.2 \pm 1.7\text{ mg}_{EMn}\text{ m}^{-2}\text{ d}^{-1}$ ,  $37.9 \pm 0.7\text{ mg}_{EMn}\text{ m}^{-2}\text{ d}^{-1}$  and  $54.5 \pm 1.8\text{ mg}_{EMn}\text{ m}^{-2}\text{ d}^{-1}$  respectively. Silicon limitation therefore stimulates EMn release, while nitrogen limitation shows the best results for EMn productivity, with  $54.5 \pm 1.8\text{ mg}_{EMn}\text{ m}^{-2}\text{ d}^{-1}$ . Note that there is no significant difference ( $t$ -test  $p = 0.376$  for  $n = 5$ ) between phosphorus and silicon limitation biomass productivity, which is not observed with  $0.57 \pm 0.05$  and  $0.62 \pm 0.08\text{ mg}_{EMn}\text{ m}^{-2}\text{ d}^{-1}$  respectively. EMn productivity is significantly higher ( $t$ -test  $p = 0.002$  for  $n = 5$ ) for silicon limitation, with  $37.9 \pm 0.7\text{ mg}_{EMn}\text{ m}^{-2}\text{ d}^{-1}$  than for phosphorus limitation, reaching only  $9.2 \pm 1.7\text{ mg}_{EMn}\text{ m}^{-2}\text{ d}^{-1}$ . The opposite situation can be observed with EMn productivity under replete culture, reaching  $5.3 \pm 0.2\text{ mg}_{EMn}\text{ m}^{-2}\text{ d}^{-1}$ , and the carbon-depleted culture, reaching  $5.8 \pm 0.6\text{ mg}_{EMn}\text{ m}^{-2}\text{ d}^{-1}$ , whereas biomass productivity for replete culture is 3.5 times higher. Finally, all these results show that nutrient limitation (especially in Si and N) leads to a more marked release of EMn, resulting in greater EMn productivity.

Since nutrient depletion is known to greatly affect cell physiology and morphology, productivity was also analyzed in terms of cells productivity as obtained from cells counting. Similar trends as with the

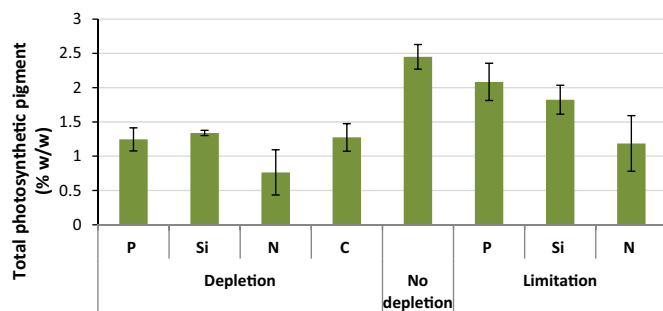


Fig. 9. Total photosynthetic pigment concentration of *Haslea ostrearia* under various nutrient limitations and depletions. Data is mean  $\pm$  SD ( $n = 5$ ).

biomass concentration were observed under both nitrogen depletion and limitation, with respectively  $4.3 \pm 0.2 \times 10^5$  and  $5.5 \pm 0.2 \times 10^5\text{ cell m}^{-2}\text{ d}^{-1}$ , which were found to be directly proportional to biomass productivity. However, in phosphorus depletion and limitation conditions, cell productivity reached respectively  $18.4 \pm 0.5 \times 10^5$  and  $9.4 \pm 0.1 \times 10^5\text{ cell m}^{-2}\text{ d}^{-1}$ , whereas biomass productivity was found to be constant ( $t$ -test  $p = 0.274$  for  $n = 5$ ) with  $0.6 \pm 0.1\text{ g}_x\text{ m}^{-2}\text{ d}^{-1}$  for P depletion and  $0.6 \pm 0.1\text{ g}_x\text{ m}^{-2}\text{ d}^{-1}$  for P limitation. As was observed between EMn and biomass productivity, nutrient depletion and limitation led then to a low correlation ( $r = 0.4178$ ) between cell and biomass productivity. This decorrelation is mainly observed in nutrient depletion for phosphorus and silicon. The observation of different cell productivities with low biomass productivities attests to a metabolism reorientation of *H. ostrearia* in depletion culture conditions. High cell density in phosphorus-depleted conditions but with 3.5 times lower mass than no-depleted culture shows that cell variation composition may be linked to metabolism adaptation [42,45,46,47].

As a conclusion to these studies, no clear correlation can be assessed between biomass and cell EMn productivity. However, it can be concluded that unrestricted culture favors biomass production, with  $1.6 \pm 0.1\text{ g}_x\text{ m}^{-2}\text{ d}^{-1}$ , and nitrogen limitation favors EMn release, with  $54.5 \pm 1.8\text{ mg}_{EMn}\text{ m}^{-2}\text{ d}^{-1}$ .

### 3.5. Towards an optimized production protocol

#### 3.5.1. EMn concentration impact on process productivity

Previous studies have exhibited differing optimal conditions ( $pH_{OPT}$ ,  $T_{OPT}$ ,  $A_{OPT}$ ) between growth and EMn production. This raises the hypothesis of EMn having a negative impact on biomass productivity (i.e. culture growth rate), and consequently on EMn productivity. Two tests were therefore carried out to identify the impact of EMn on productivity.

*H. ostrearia* was cultivated in semi-continuous mode to remove 90% of culture medium at each culture medium renewal, taking advantage of the benthic cell characteristics. For this purpose, stirring was stopped a few hours before culture renewal to allow the cells to sediment at the bottom of the PBR, and culture was renewed by pumping culture medium from the top of the culture volume before replacing it with fresh medium.

Two residence times were used: 10 days and 5 days, corresponding to around  $D = 0.09\text{ d}^{-1}$  and  $D = 0.18\text{ d}^{-1}$  respectively. The experiments were done with an optimized formulation of NX medium to avoid Si, P and C fed-batch strategy. The cultures were carried out in a 1 L airlift PBR. The temperature of the culture was fixed at  $22\text{ }^{\circ}\text{C}$ , pH regulation at 7.8 and incident PFD at  $300\text{ }\mu\text{mol m}^{-2}\text{ s}^{-1}$  (to obtain  $A_{OPT} = 12\text{ }\mu\text{mol}_{hv}\text{ g}_x^{-1}\text{ s}^{-1}$ ) in the day/night cycle 14/10. For the first part of the study, *H. ostrearia* was cultivated under nitrogen limitation (NX-5N100P6Si) conditions in order to enhance marennine production, according to results achieved in the previous section. Results are given in Fig. 11.

After 10 days, cell density reached  $4 \pm 0.1 \times 10^8\text{ cell L}^{-1}$ , which also corresponds to maximum EMn concentration ( $11\text{ mg}_{EMn}\text{ L}^{-1}$ , Fig. 11-A). Culture medium was then renewed at 90%. As expected, this resulted in a marked decrease in EMn concentration due to the dilution (around  $2\text{ mg}_{EMn}\text{ L}^{-1}$ ). Similar observation can be made on day 20, when the second medium renewal was applied. After 10 days of EMn accumulation in the culture medium, the concentration was decreased by culture renewal. However, this also induced a continuous decrease in cell density over time. Even though the cell should have been immobilized at the bottom of the PBR during the sample step, some of the cells were definitely sampled during medium renewal. Cell density decreased to finally reach  $0.4 \pm 0.1 \times 10^8\text{ cell L}^{-1}$  by day 31. In addition, EMn concentration was found to remain below  $11.6 \pm 0.1\text{ mg}_{EMn}\text{ L}^{-1}$  and decrease greatly over time, reaching  $5.7 \pm 0.3\text{ mg}_{EMn}\text{ L}^{-1}$  at day 31.

The same observation was made for the 5 days' residence time experiment (Fig. 11-B). EMn concentration increased between each culture renewal, reaching  $4.3 \pm 0.1\text{ mg}_{EMn}\text{ L}^{-1}$  and  $5 \pm 0.1\text{ mg}_{EMn}\text{ L}^{-1}$  at day 10 and day 15 respectively, but then decreased over the culture to

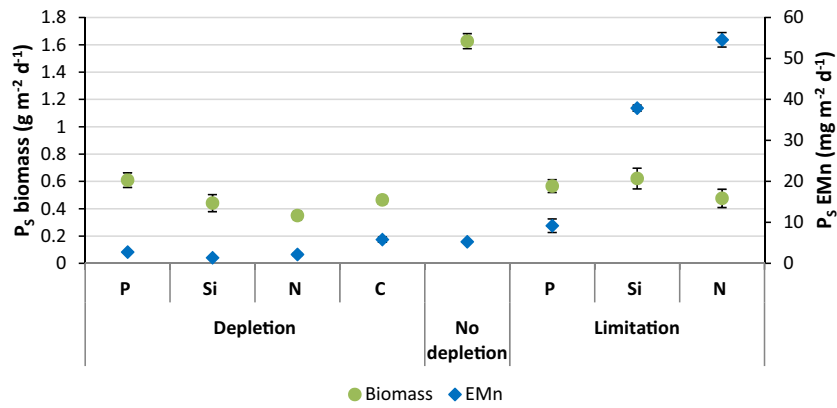


Fig. 10. Biomass and EMn productivity of *Haslea ostrearia* culture under various nutrient limitations and depletions. Data is mean  $\pm$  SD (n = 5).

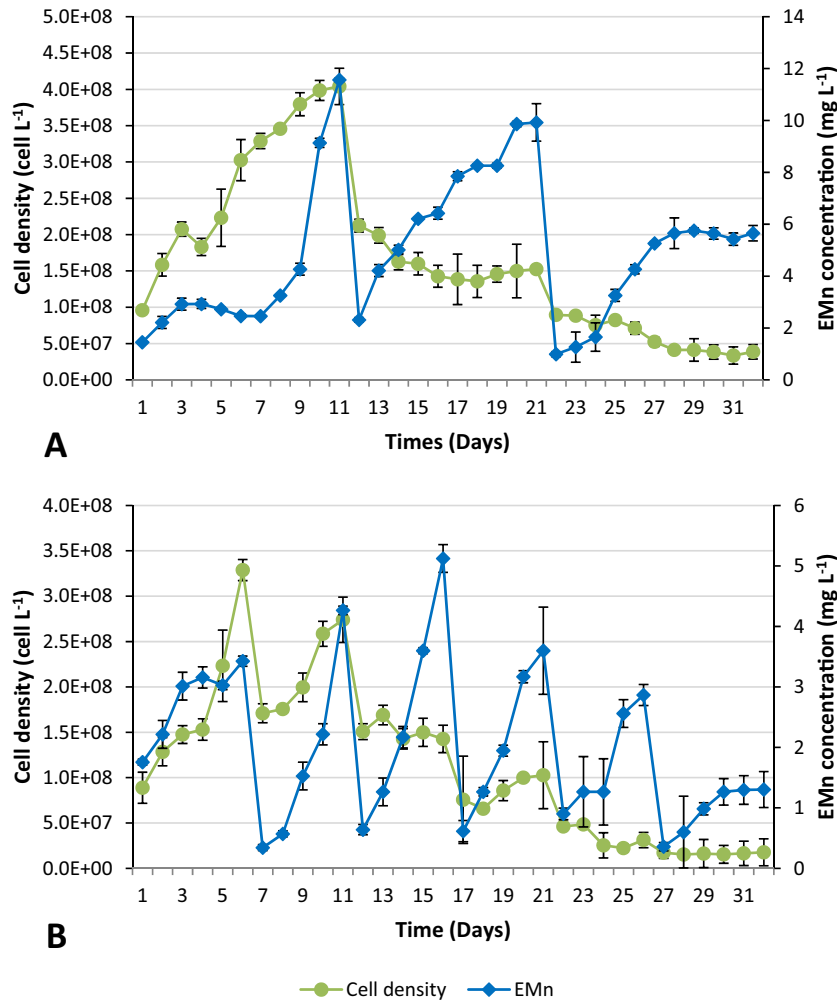


Fig. 11. Evolution of cell density and extracellular marennine concentration (EMn) for semi-continuous culture of *Haslea ostrearia* in NX medium in 1 L airlift PBR (Panel A with  $D = 0.09 \text{ d}^{-1}$ , corresponding to 10 days of residence time – Panel B with  $D = 0.18 \text{ d}^{-1}$  corresponding to 5 days of residence time). Data is mean  $\pm$  SD (n = 3).

reach  $1.3 \pm 0.3 \text{ mg}_{\text{EMn}} \text{ L}^{-1}$  by day 31. In terms of cell density, each medium renewal reduced it and the cells barely managed any growth. Cell density reached  $3.3 \pm 0.1 \times 10^8 \text{ cell L}^{-1}$  by day 5 and finally decreased to  $1.7 \pm 0.1 \times 10^7 \text{ cell L}^{-1}$ .

Comparing the two experiments, the 10 days' residence time experiment and 5 days' residence time experiment led to an average EMn productivity of  $1.0 \text{ mg}_{\text{EMn}} \text{ L}^{-1} \text{ d}^{-1}$  and  $0.7 \text{ mg}_{\text{EMn}} \text{ L}^{-1} \text{ d}^{-1}$

respectively. Both these productivities are lower than the results obtained by Rossignol [13]. In addition, no stable production was obtained for any of these tests. The dilution step led to progressive cell density decrease, although EMn concentration was regularly decreased. There was no strong evidence of any relationship between EMn concentration and biomass productivity. However, a progressive evolution of *H. ostrearia* cell population was observed, which was found to be



transfer of CO<sub>2</sub> in the biofilm.

A systematic optimization was then conducted in cell-suspended mode. Dissolved inorganic carbon (DIC) was added by CO<sub>2</sub> injection, eventually combined with the addition of sodium bicarbonate (Figs. 4–6). Increasing DIC was found to increase *H. ostrearia* growth, with a significant effect on EMn production, reaching 7.3 mg L<sup>-1</sup> with 15% CO<sub>2</sub> against 1.0 mg L<sup>-1</sup> with 2% CO<sub>2</sub>. This could be attributed to the carbon content (36 ± 0.6%) of EMn which could request a sufficient carbon supply for its synthesis [24]. With the addition of sodium bicarbonate, it was found necessary to keep DIC constant at 10 mM, to reach 31.7 ± 0.3 mg L<sup>-1</sup> d<sup>-1</sup> of biomass and 0.8 ± 0.1 mg L<sup>-1</sup> d<sup>-1</sup> of EMn in semi-continuous culture mode. However, culture medium precipitation appeared at high DIC, phosphorus and silicon concentration, which impaired biomass and EMn productivity.

The substrate consumption rate  $H_c$  ( $r_s$ ) and specific substrate consumption rates ( $Q_s$ ) of NO<sub>3</sub><sup>-</sup>, PO<sub>4</sub><sup>3-</sup> and SiO<sub>3</sub><sup>2-</sup> (Table 1) were determined. This enabled us to set a fed-batch strategy for the P, Si, C elements, avoiding precipitation and therefore increasing biomass productivity to 51.8 ± 2.3 mg<sub>X</sub> L<sup>-1</sup> d<sup>-1</sup>. In terms of EMn productivity, this leads to the lowest productivity obtained, with 0.2 ± 0.1 mg<sub>EMn</sub> L<sup>-1</sup> d<sup>-1</sup> (Fig. 6). As described by Robert [20], *H. ostrearia* excretes marennine continuously, but surprisingly in nutrient unrestricted conditions this leads to metabolism orientation to reduce EMn production. As described in previous studies [21,13,14], marennine overproduction can be induced by nitrogen limitation. This was confirmed by our study (Fig. 9–10). Phosphorus, silicon and nitrogen limitation conditions lead to higher productivities than the control test, respectively 9.2 ± 1.7 mg<sub>EMn</sub> m<sup>-2</sup> d<sup>-1</sup>, 37.9 ± 0.7 mg<sub>EMn</sub> m<sup>-2</sup> d<sup>-1</sup> and 54.5 ± 1.8 mg<sub>EMn</sub> m<sup>-2</sup> d<sup>-1</sup>. Nitrogen is definitely the best nutrient limitation to overproduce EMn.

Optimal conditions of temperature, pH and light were investigated. pH<sub>OPT</sub> = 7.8 and T<sub>OPT</sub> = 22 °C were assessed (Fig. 8). These values were not different from the ideal settings previously established [20,48], but it was found quite difficult to determine the optimal ones due to the medium chemistry leading to precipitation of the medium, which started at pH 8 and 25 °C [43].

Concerning light, it was determined here to be a function of the MRPA (denoted A), which enables PFD, biomass concentration and PBR geometry to be gathered in a single representative physical quantity. Different optimal values A<sub>OPT</sub> were identified for both biomass and EMn production, with respectively 1.7 ± 0.1 g<sub>X</sub> m<sup>-2</sup> d<sup>-1</sup> at 12.3 μmol<sub>hv</sub> g<sub>X</sub><sup>-1</sup> s<sup>-1</sup> and 11.0 ± 0.6 mg<sub>EMn</sub> m<sup>-2</sup> d<sup>-1</sup> at 8.4 μmol<sub>hv</sub> g<sub>X</sub><sup>-1</sup> s<sup>-1</sup> (Fig. 7). Biomass production was found to be positively impacted by high PFD until an MRPA of around 12 μmol<sub>hv</sub> g<sub>X</sub><sup>-1</sup> s<sup>-1</sup> was reached. We also noted that these values were close to the values for other species known for their high light tolerance (*Chlorella vulgaris* and *Nannochloropsis gaditana*, with 15 μmol<sub>hv</sub> g<sub>X</sub><sup>-1</sup> s<sup>-1</sup> ≥ A<sub>OPT</sub> ≤ 20 μmol<sub>hv</sub> g<sub>X</sub><sup>-1</sup> s<sup>-1</sup> and A<sub>OPT</sub> = 13 μmol<sub>hv</sub> g<sub>X</sub><sup>-1</sup> s<sup>-1</sup> respectively) [44].

The conversion efficiency of light into biomass (Fig. 7) showed an efficiency of around 0.10 ± 0.01 g<sub>X</sub> mol<sub>hv</sub><sup>-1</sup> for MRPA values in the range 8–12 μmol<sub>hv</sub> g<sub>X</sub><sup>-1</sup> s<sup>-1</sup>, but a low correlation (r = 0.4564) between MRPA and total pigment concentration evolution was observed. The lower the MRPA value, the higher the pigment concentration should be, according to the photoadaptation phenomenon [49,44]. The reverse behavior was observed here for *H. ostrearia*, with an increase in photosynthetic pigment content from 8 to 12 μmol<sub>hv</sub> g<sub>X</sub><sup>-1</sup> s<sup>-1</sup>, which was also found to correspond to the maximum conversion efficiency of light into biomass. This also corresponded to a simultaneous decrease in EMn concentration (%) with a switch from EMn production to biomass, which could be estimated at around 8 μmol<sub>hv</sub> g<sub>X</sub><sup>-1</sup> s<sup>-1</sup> (Fig. 7). All these results tend to indicate a possible particular evolution of *H. ostrearia* pigments towards light (i.e. different from *Chlorophyceae*), which could be linked to *H. ostrearia* metabolism.

In terms of EMn production, a productivity of 11.0 ± 0.6 mg<sub>EMn</sub> m<sup>-2</sup> d<sup>-1</sup> produced at 8.4 μmol<sub>hv</sub> g<sub>X</sub><sup>-1</sup> s<sup>-1</sup> was obtained. Light, as represented by the MRPA, was revealed to be an important parameter for marennine production. But contrary to Mouget et al. [50,51], according to whom

the higher the PFD, the higher the EMn produced, our study showed an optimal MRPA for EMn production at around 8 μmol<sub>hv</sub> g<sub>X</sub><sup>-1</sup> s<sup>-1</sup>, which was found to be lower than the optimal MRPA for biomass production. Given that the origin of marennine synthesis is still unknown, only a partial hypothesis can be elaborated here. In our experiments, EMn production was found to be inversely related to biomass productivity and photosynthetic pigment concentration (Figs. 7–8). Even if EMn could (directly or indirectly) come from photosynthetic pigment synthesis or be related to photosynthetic growth metabolism, it certainly follows its own pathway and role in terms of cell physiology. These pathways could be energetically in conflict. Therefore, the cell should promote either biomass or marennine. This hypothesis tends to be verified by our experiment with nitrogen limitation conditions, which revealed the enhancement of EMn synthesis.

EMn is known to be a highly bioactive molecule [10]. Therefore, when concentration is increased in culture it could have a negative impact on *H. ostrearia* growth. If marennine has a negative impact on biomass productivity (and thus the EMn synthesis itself) during the production process, this molecule should be removed from the medium during culture. Additionally, the shadowing characteristic of EMn also raises the possibility of limiting light propagation in the PBR, thus also reducing photosynthetic growth. We therefore tested an adapted protocol based on medium renewal (+EMn) after a period of unstirred conditions to allow cells to sediment at the bottom of the PBR (Fig. 11). Unfortunately, the tychoelagic characteristic of the cell prevented it from removing 90% of EMn without decreasing too much cell density. The hypothesis of controlling the tychoelagic behavior by culture condition is raised to better control the production process.

In a final experiment, we finally demonstrated that whatever the impact of marennine, the culture of *H. ostrearia* in a stirred conventional PBR managed to produce continuous EMn at 4.5 ± 0.16 mg<sub>EMn</sub> L<sup>-1</sup> d<sup>-1</sup>, against 0.7 ± 0.1 mg<sub>EMn</sub> L<sup>-1</sup> d<sup>-1</sup> for immobilized cell culture (Fig. 12). The conventional stirred PBR is therefore confirmed for *H. ostrearia* culture and continuous EMn production.

## 5. Conclusions

Cell immobilization has been presented as a solution for *H. ostrearia* culture for a long time [20,15,16,52,13,14,53]. However, it is rather difficult to scale up and induces possible limitations related to mass or even light transfer in biofilms [54,55,56,57,25]. In the case of *H. ostrearia*, the composition of the culture medium is prone to chemical precipitation, which could limit biomass and EMn productivity. It was then found difficult to fully optimize pH and temperature because of their relationship with the precipitation phenomenon. Further improvement of the culture medium and conditions (being related) is still possible. The use of P, Si and C fed-batch was found to be a useful strategy and could be used for this purpose.

Among the various parameters, light as represented by the MRPA was found to be highly relevant. It impacts biomass productivity and also EMn synthesis, pigment and overall conversion efficiency. However, the particular response to low MRPA value remains to be further investigated, as its behavior towards pigment evolution was found different between EMn and other pigments. Hypothetically, this bias in cell response could come from the EMn synthesis and be confirmed by the study of EMn production to light conditions.

The marennine synthesis pathway was not elucidated in our study (as this was not the main aim of this work), but it was confirmed that continuous EMn production and excretion occur in a PBR culture, even without nutrient limitation. Overproduction was obtained by applying silicate or nitrogen limitation. As a consequence, nutrient concentration variation and its consequences for culture cell physiology remains to be investigated.

To conclude, once all optimum parameters are collected and applied, the culture of *H. ostrearia* cells in a stirred airlift PBR is possible. We succeeded in scaling up *H. ostrearia* culture to a 6 L PBR and an EMn

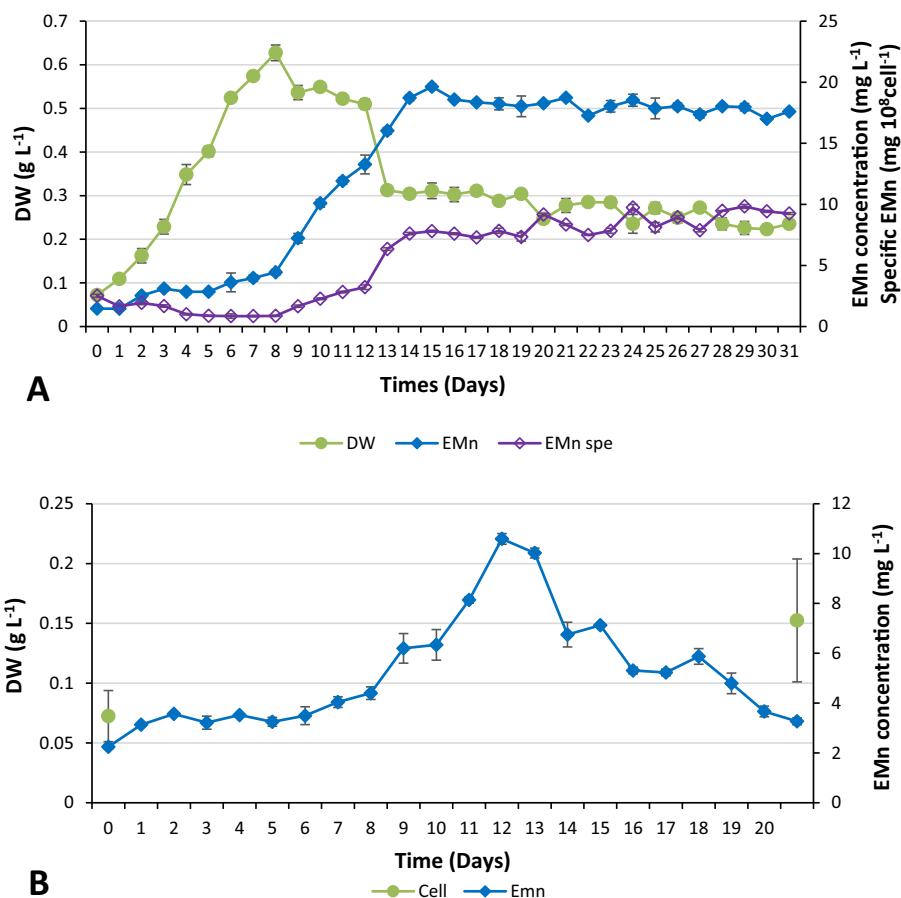


**Fig. 12.** Evolution of dry weight (DW), extracellular marennine concentration (EMn) and specific EMn concentration of *Haslea ostrearia* for semi-continuous culture in NX media with optimal culture conditions in a 1 L airlift PBR (Panel A) and for a continuous culture in NX media with optimal culture conditions in a 500 mL immobilized cell PBR (Panel B). Data is mean  $\pm$  SD (n = 3).

productivity of  $4.5 \pm 0.2 \text{ mg}_{\text{EMn}} \text{ L}^{-1} \text{ d}^{-1}$  was achieved against  $0.7 \pm 0.1 \text{ mg}_{\text{EMn}} \text{ L}^{-1} \text{ d}^{-1}$  for immobilized cell culture. The NX medium was found to be stable at pH 7.8 and the P, Si, C fed-batch could be avoided.

Such results suggest a possible protocol for increased production of EMn from *H. ostrearia*. Using, for example, membrane technology, the suspended pelagic cells could be retained in the culture volume while allowing continued recovery of the EMn produced in the mixed PBR.

#### CRediT authorship contribution statement

**R. Nghiem Xuan:** Conceptualization, Investigation, Methodology, Formal analysis, Writing – original draft. **J.L. Mouget:** Validation, Visualization, Supervision. **V. Turpin:** Validation, Visualization, Supervision. **P. Jaouen:** Validation, Visualization, Supervision, Funding acquisition. **J. Pruvost:** Validation, Conceptualization, Supervision, Formal analysis, Methodology, Writing – review & editing.

#### Declaration of competing interest

The authors declare that they have no known competing financial interests or personal relationships that could have appeared to influence the work reported in this paper.

#### Acknowledgements

We are very grateful to the AMI (Atlantic Microalgae) scientific consortium and the Pays de la Loire region (France), who have supported our research. This publication has also benefited from European

Commission funding under the Horizon 2020 Research and Innovation Program GHANA (The Genus *Haslea*, New marine resources for blue biotechnology and Aquaculture). We would also like to acknowledge H el ene Marec and Emmanuel Dechandol for the instrumentation and implementation of the culture system. We would like to thank Vladimir Heredia Marquez, J er emy Monlyade and Alexandra Busnel for their constant constructive discussions.

#### Statement of informed consent

We state that no conflicts, informed consent, human or animal rights applicable.

#### Funding

European Commission under the Horizon 2020 Research and Innovation Program GHANA (The Genus *Haslea*, New marine resources for blue biotechnology and Aquaculture, grant agreement No [734708/GHANA/H2020-MSCA-RISE- 2016]).

#### Appendix A. Supplementary data

Supplementary data to this article can be found online at <https://doi.org/10.1016/j.algal.2021.102251>.

## References

- [1] P. Spolaore, C. Joannis-Cassan, E. Duran, A. Isambert, Commercial applications of microalgae, *J. Biosci. Bioeng.* 101 (2) (2006) 87–96, <https://doi.org/10.1263/jbb.101.87>.
- [2] Cardozo K. H-M, T. Guaratini, M.P. Barros, V.R. Falcão, A.P. Tonon, N.P. Lopes, S. Campos, M.A. Torres, A.O. Souza, P. Colepicolo, E. Pinto, Metabolites from algae with economical impact, *Comp. Biochem. Physiol.* 146 (1–2) (2007) 60–78, <https://doi.org/10.1016/j.cbpc.2006.05.007>. C. Elsevier Inc.
- [3] Starck S. (2012). A place in the sun - Algae is the crop of the future, according to researchers in Geel, *Flanders Today*, Retrieved 8 December 2012.
- [4] C. Wang, C.Q. Lan, Effects of shear stress on microalgae – a review, *Biotechnol. Adv.* 36 (4) (2018) 986–1002, <https://doi.org/10.1016/j.biotechadv.2018.03.001>.
- [5] M.R. Shah, Y. Liang, J.J. Cheng, M. Daroch, Astaxanthin-producing green microalga *Haematococcus pluvialis*: from single cell to high value commercial products, *Front. Plant Sci.* 7 (2016) 531, <https://doi.org/10.3389/fpls.2016.00531>.
- [6] G. Panis, J.R. Carreon, Commercial astaxanthin production derived by green alga *Haematococcus pluvialis*: a microalgae process model and a techno-economic assessment all through production line, *Algal Res.* 18 (2016) 175–190, <https://doi.org/10.1016/j.algal.2016.06.007>.
- [7] A. Ben-Amotz, M. Avron, Accumulation of metabolites by halotolerant algae and its industrial potential, *Annu. Rev. Microbiol.* 37 (1983) 95–119, <https://doi.org/10.1146/annurev.mi.37.100183.000523>.
- [8] A. Oren, A hundred years of *Dunaliella* research: 1905–2005, *Saline Syst.* 1 (2005) 2, <https://doi.org/10.1186/1746-1448-1->.
- [9] B. Gaillon, Des huîtres vertes, et des causes de cette coloration, *J. Phys. Chim. Hist. Nat. Arts* 91 (1820) 222–225.
- [10] Gastineau R., Pouvreau J-B., Helliou C., Morancais M., Gaudin P., Bourgougnon N., Mouget J-L. (2012). Biological activities of purified marennine, the blue pigment responsible for the greening of oysters. *J. Agric. Food Chem.* 60(14):3599–605. doi: <https://doi.org/10.1021/jf205004x>.
- [11] Gastineau, R.; Turcotte, F.; Pouvreau, J.; Morancais, M.; Fleurence, J.; Windarto, E.; Prasetiva, F. S.; Arsad, S.; Jaouen, P.; Babin, M.; Coiffard, L.; Couteau, C.; Bardeau, J-F.; Jaquette, B.; Leignel, V.; Hardivillier, Y.; Marcotte, I.; Bourgougnon, N.; Tremblay, R.; Deschènes, J.-S.; Badawy, H.; Pasetto, P.; Davidovich, N.; Hansen, G.; Dittmer, I.; Mouget, J.-L. (2014). Marennine, promising blue pigments from a widespread *Haslea* diatom species complex. *Mar. Drugs*, 12, 3161–3189.
- [12] L. Vandanjon, N. Rossignol, P. Jaouen, J.M. Robert, F. Quéméneur, Effect of shear on two microalgae species. Contribution of pumps and valves in tangential flow filtration systems, *Biotechnology and Bioengineering* 63 (1) (1999) 1–9, [https://doi.org/10.1002/\(SICI\)1097-0290\(19990405\)63:1<1::AID-BIT1>3.0.CO;2-K](https://doi.org/10.1002/(SICI)1097-0290(19990405)63:1<1::AID-BIT1>3.0.CO;2-K).
- [13] Rossignol N. (1999). Procédés d'extraction et de séparation par membranes appliqués à la production du pigment endo-et extracellulaire synthétisé par la diatomée *Haslea ostrearia* Simonsen. Mise en oeuvre d'un photobioréacteur à membranes à fonctionnement continu. (Thèse de doctorat ; Université de Nantes).
- [14] T. Lebeau, P. Gaudin, G.-A. Junter, L. Mignot, Robert J-M, Continuous marennin production by agar-entrapped *Haslea ostrearia* using a tubular photobioreactor with internal illumination, *Appl. Microbiol. Biotechnol.* 54 (2000) 634–640.
- [15] Robert J-M. (1989). Procédé de culture en masse de la diatomée *Haslea ostrearia* Simonsen. European and French patent no 8915314. Nantes University.
- [16] Rouillard I. (1996). Optimisation de la production en masse d'*Haslea ostrearia* Simonsen sur une eau souterraine salée: importance de la souche et des conditions de culture; comparaison avec *Skeletonema costatum* (Grev) Cleve. (Thèse de doctorat ; Université de Nantes).
- [17] R. Nghiem Xuan, I. Safitri, J.L. Mouget, J. Pruvost, V. Turpin, P. Jaouen, Design of artificial culture medium to optimize *Haslea ostrearia* biomass and marennine production, *Algal Res.* 45 (2019) 101653. Elsevier, 2020.
- [18] Pruvost J., Van Vooren G., Cogne G., Legrand J. (2009). Investigation of biomass and lipids production with *Nochloris oleoabundans* in photobioreactor. *Bioresour. Technol.* 100 (23): 5988–95.
- [19] Takache H., Pruvost J., Cornet J-F. (2012). Kinetic modeling of the photosynthetic growth of *Chlamydomonas reinhardtii* in a photobioreactor. *Biotechnol. Prog.*, 28 (3): 681–92.
- [20] J-M. Robert, Fertilité des claires ostréicoles et verdissement: utilisation de l'azote par les diatomées dominantes, in: (Thèse de Doctorat : Université de Nantes), 1983.
- [21] D. Neuville, P. Daste, Production du pigment bleu par la diatomée *Navicula ostrearia* (Gaillon) Bory, maintenue en culture uni-algae sur milieu synthétique carencé en azote, *C. R. Acad. Sci. Paris* 374 (1972) 2030–2033.
- [22] R.J. Ritchie, Universal chlorophyll equations for estimating chlorophylls *a*, *b*, *c*, and *d* and total chlorophylls in natural assemblages of photosynthetic organisms using acetone, methanol, or ethanol solvents, *Photosynthetica* 46 (1) (2008) 115–126.
- [23] J.D. Strickland, T. Parsons, A practical handbook of seawater analysis, in: *Fisheries Research Bulletin*, Bd, Canada, 1968.
- [24] Pouvreau J-B, E. Morancais, F. Fleury, P. Rosa, L. Thion, B. Cahingt, Preliminary characterisation of the blue-green pigment "marennine" from the marine tychoepelagic diatom *Haslea ostrearia* (Gaillon/Bory) Simonsen, *J. Appl. Phycol.* 18 (2006) 757–767, <https://doi.org/10.1007/s10811-006-9087-x>.
- [25] K. Grasshoff, K. Kremling, L.G. Anderson, M.O. Andreae, B. Behrends, B. Yhlen, *Methods of Seawater Analysis*, WILEY-VCH Verlag GmbH. Revised Completely, 2007.
- [26] Cornet J-F, C.G. Dussap, Gros J-B, Kinetics and energetics of photosynthetic microorganisms in photobioreactors, in: *Bioprocess and Algae Reactor Technology*, Apoptosis, *Advances in Biochemical Engineering Biotechnology*, 59, Springer, Berlin Heidelberg, 1998, pp. 153–224.
- [27] J. Pruvost, J-F. Cornet, J. Legrand, Hydrodynamics influence on light conversion in photobioreactors: an energetically consistent analysis, *Chem. Eng. Sci* 63 (14) (2008) 3679–3694.
- [28] R. Kandilian, J. Pruvost, J. Legrand, L. Pilon, Influence of light absorption rate by *Nannochloropsis oculata* on triglyceride production during nitrogen starvation, *Bioresour. Technol.* 163 (July) (2014) 308–319.
- [29] L. Pilon, H. Berberoglu, R. Kandilian, Radiation transfer in photobiological carbon dioxide fixation and fuel production by microalgae, *J. Quant. Spectrosc. Radiat. Transf* 112 (17) (2011) 2639–2660.
- [30] R. Kandilian, J. Pruvost, A. Artu, C. Lemasson, J. Legrand, L. Pilon, Comparison of experimentally and theoretically determined radiation characteristics of photosynthetic microorganisms, *J. Quant. Spectrosc. Radiat. Transf.* 175 (2016) 30–45. <https://doi.org/10.1016/j.jqsrt.2016.01.031>.
- [32] M. Ndiaye, E. Gadoin, C. Genric, CO<sub>2</sub> gas-liquid mass transfer and kLa estimation: numerical investigation in the context of airlift photobioreactor scale-up, *Chem. Eng. Res. Des.* 133 (2018) 90–102.
- [33] Y. Chisti, M. Moo-Young, Calculation of shear rate and apparent viscosity in airlift and bubble column bioreactors, *Biotechnol. Bioeng.* 34 (1989) 0–1.
- [34] A. Contreras, F. Garcia, E. Molina, J.C. Merchuk, Interaction between CO<sub>2</sub>-mass transfer, light availability, and hydrodynamic stress in the growth of *Phaeodactylum tricornutum* in a concentric tube airlift photobioreactor, *Biotechnol. Bioeng.* 60 (1998) 317–325.
- [35] M.J. Barbosa, Hadiyanto, R.H. Wijffels, Overcoming shear stress of microalgae cultures in sparged photobioreactors, *Biotechnol. Bioeng.* 85 (2004) 78–85, <https://doi.org/10.1002/bit.10862>.
- [36] M.H.A. Michels, J. Atze, J. Van Der Goot, N.-H.R. Norsker, R.H. Wijffels, Effects of shear stress on the microalgae *Chaetoceros muelleri*, *J. Appl. Phycol.* 28 (1) (2010) 53–62, <https://doi.org/10.1007/s00449-010-0415-9>.
- [37] T.M. Sobczuk, F.G. Camacho, E.M. Grima, Y. Chisti, Effects of agitation on the microalgae *Phaeodactylum tricornutum* and *Porphyridium cruentum*, *Bioprocess Biosyst. Eng.* 28 (2006) 243–250.
- [38] B. Moutel, Étude de l'intérêt pharmaceutique et d'une production industrielle des lipides issus de la microalgue *Botryococcus braunii*, Thèse de doctorat, Université de Nantes, 2016.
- [39] B. Le Guic, H. Marec, J. Pruvost, J.F. Cornet, Investigation of growth limitation by CO<sub>2</sub> mass transfer and inorganic carbon source for the microalga *Chlorella vulgaris* in a dedicated photobioreactor, *Chem. Eng. Sci.* 233 (2021), 116388.
- [40] B.J. Shel, D.T. Canvin, Utilization of exogenous inorganic carbon species in photosynthesis by *Chlorella pyrenoidosa*, *Plant Physiol.* 65 (1980) 774–779.
- [41] G.G. Bozzo, B. Colman, Y. Matsuda, Active transport of CO<sub>2</sub> and bicarbonate is induced in response to external CO<sub>2</sub> concentration in the green alga *Chlorella kessleri*, *J. Exp. Bot.* 51 (2000) 1341–1348.
- [42] G.W. Morey, R. Fournier, J. Rowe, The solubility of amorphous silica at 25°C, *J. Geophys. Res.* 69 (10) (1995) 1995–2002.
- [43] T.D. Nguyen, M. Frappart, P. Jaouen, J. Pruvost, P. Bourseau, Harvesting *Chlorella vulgaris* by natural increase in pH: effect of medium composition, *Environ. Technol* 35 (9–12) (2014) 1378–1388.
- [44] Artu A. (2016).: Etude et optimisation de la culture de microalgues en photobioréacteurs solaires. (Thèse de doctorat ; Université de Nantes).
- [45] L. Rodolfi, G. Chini Zittelli, N. Bassi, G. Padovani, N. Biondi, G. Bonini, Microalgae for oil: strain selection, induction of lipid synthesis and outdoor mass cultivation in a low-cost photobioreactor, *Biotechnol. Bioeng.* 102 (2009) 100–112. <https://doi.org/10.1002/bit.22033>.
- [46] K. Goiris, W. Van Colen, I. Wilches, F. León-Tamariz, L. De Cooman, K. Muylaert, Impact of nutrient stress on antioxidant production in three species of microalgae, *Algal Res.* 7 (2015) 51–57.
- [47] K. Bajwa, N.R. Bishnoi, A. Kirrolia, S. Tamil Selvan, Evaluation of nutrient stress (nitrogen, phosphorus regimes) on physio-biochemical parameters of oleaginous microalgal strains and SEM study under nutrient stress, *Int. J. Environ. Sci. Nat. Resour.* 10 (1) (2007), <https://doi.org/10.19080/IJESNR.2018.10.555776>.
- [48] V. Turpin, Robert J-M, P. Gouletquer, Limiting nutrients of oyster pond seawaters in the Marennes-Oléron region for *Haslea ostrearia*: applications to the mass production of the diatom in mesocosm experiments, *Aquat. Living Resour.* 12 (1999) 335–342.
- [49] J. Pruvost, Cornet J-F, Knowledge models for the engineering and optimization of photobioreactors, in: *Microalgal Biotechnology: Potential and Production*, De Gruyter, Berlin, Germany, 2012, pp. 181–224.
- [50] Mouget J-L, P. Rosa, G. Tremblin, Acclimation of *Haslea ostrearia* to light of different spectral qualities – confirmation of "chromatic adaptation" in diatoms, *J. Photochem. Photobiol.* 19;75 (1–2) (2004) 1–11, <https://doi.org/10.1016/j.jphotobiol.2004.04.002>.
- [51] Mouget J-L, P. Rosa, C. Vachoux, G. Tremblin, Enhancement of marennine production by blue light in the diatom *Haslea ostrearia*, *J. Appl. Phycol.* 17 (5) (2005) 437–445, <https://doi.org/10.1007/s10811-005-0561-7>, 437–44517.
- [52] Y. Rincé, T. Lebeau, J.M. Robert, Artificial cell-immobilization: a model simulating immobilization in natural environments? *J. Appl. Phycol.* 11 (1999) 263–272.
- [53] V. Turpin, Robert J-M, P. Gouletquer, G. Massé, P. Rosa, Oyster greening by outdoor mass culture of the diatom *Haslea ostrearia* Simonsen in enriched seawater, *Aquac. Res.* 32 (801–809) (2001).
- [54] W.L. Hochfeld, *Producing Biomolecular Substances With Fermenters, Bioreactors, and Biomolecular Synthesizers*, Taylor & Francis, Boca Raton, FL, 2005. ISBN 9781420021318.
- [55] J.C. Gabelle, E. Jourdir, R. Licht, F. Ben Chaabane, I. Henaut, J. Mochain, F. Augier, Impact of rheology on the mass transfer coefficient during the growth

phase of *Trichoderma reesei* in stirred bioreactors, *Chem. Eng. Sci.* 75 (2012) 408–417, <https://doi.org/10.1016/j.ces.2012.03.053>.

[56] A. Souliès, Contribution à l'étude hydrodynamique et à la modélisation des photobioréacteurs à haute productivité volumique, Thèse de doctorat, Université de Nantes, 2014.

[57] R. Kandilian, J. Bruno, J. Legrand, L. Pilon, J. Pruvost, Light transfer in agar immobilized microalgae cell cultures, *J. Quant. Spectrosc. Radiat. Transf.* 198 (2017) 81–92.